Different Data, Different General Circulations? A Comparison of Selected Fields in NCEP/DOE AMIP-II and ECMWF ERA-40 Reanalyses

by

Richard Grotjahn

Department of Land, Air, and Water Resources,
University of California, Davis, 95616, U.S.A.

6 March 2006

A submission for a special issue
of Dynamics of Atmospheres and Oceans
on the General Circulation of the Atmosphere

Abstract

Reanalysis datasets have been very popular for understanding the general circulation as well as verifying general circulation models. The most recent versions of datasets prepared by ECMWF ("ERA40") and NCEP ("NDRa2") are examined in this article. Primary variables that both relate to the atmosphere's general circulation and are readily available are compared and contrasted. Significant differences are found in the primary circulation variables and energetics. Kinetic energy is greater in ERA40 data. The surface energy budgets differ in that ERA40 data have greater sensible heat flux into the air, while NDRa2 data have greater latent heat flux. The result is NDRa2 has more moisture in the subtropics. Geographically, the two datasets have notable differences in their treatment of the intertropical convergence zone (ICZ). The ICZ over the Atlantic and eastern Pacific is narrower and stronger in ERA40 data; this causes ERA40 data to have more moisture in the tropics. The ICZ over the western Pacific and Indian ocean is generally stronger in NDRa2 data. Both datasets have a double ICZ in the western half of the Pacific in DJF; in JJA ERA40 retains that double ICZ but NDRa2 largely does not. Beyond the handling of the ICZ, the datsets differ in tropical zonal mean zonal wind, wherein ERA40 data in DJF has zonal mean upper troposphere tropical westerlies; this difference may imply a different amount of interhemispheric communication. The datasets also have strong disagreements in regions of large-scale higher topography.

1. Introduction

In recent years operational centers at the European Centre for Medium Range Weather Forecasts (ECMWF) and the U.S. National Center for Environmental Prediction (NCEP) have made a huge effort to produce uniform, long period observational datasets. The initial, widely used data sets are “ERA15”: a 15 year climatology from December 1978 through February 1994 produced by ECMWF and “NNRa1”: the NCEP/NCAR Reanalysis, a climatology starting from January 1948. These ‘precursor’ datasets have been succeeded by newer datasets: “ERA40”: an ECMWF dataset covering the period from September 1957 through August 2002, and “NDRa2”: a NCEP DOE Reanalysis 2 dataset, covering the period starting from January 1979 as of this writing.

Observations are taken at many locations but those data must be interpolated to a regular grid. The objective analysis depends on a first guess that comes from a global model. Using the same global model to process the entire record helps improve the uniformity of each dataset, but does not guarantee it because the observations themselves evolve over the record. Perhaps the largest change is from data taken before and after the advent of large amounts of satellite data, starting in December 1978. It is well known that the NNRa1 climatology of the NCEP dataset is noticeably different before and after 1978 (e.g. Kistler, et al, 2001, p. 252; Trenberth and Smith, 2005). For that reason this report will focus only on the satellite era, restricting attention to data starting after December 1978. Since different models and objective analysis techniques were used at ECMWF and NCEP, the reanalysis datasets are not the same even though most of the observations input are the same. There is some evidence (Renwick, 2003) that the differences between ERA40 and NNRa1, for at least some variables, is less after 1979 as well.

The data are most likely to be commonly used after interpolation to standard levels (instead of model levels) and to an equally-spaced grid in latitude and longitude (2.5 degree interval) instead of the model’s grid or spectral coefficients. Since that will be the common usage, the comparisons made here also use such interpolated data. For example, NCEP reanalyses are originally spectral coefficients truncated at T62 in the horizontal and 28 sigma (terrain-following) levels in the vertical. Here we use the 2.5 degree grid at 17 standard isobaric levels as provided by NCEP. Similar comments apply to the ECMWF data.

This article has a highly restricted purpose. The purpose of this article is to document similarities and differences between two datasets that are likely to be heavily used in the near future. The ECMWF ERA40 reanalysis (Uppala, et al., 2005) will be compared with the NCEP/DOE NDRa2 data (Kalnay, et al., 1996; Kanamitsu, et al., 2002). This article will ***not*** attempt to evaluate which dataset is "more correct" such an evaluation is outside the intended scope of this work. However, a few studies are cited here that have discussed the relative merits of the *precursor* datasets in certain restricted situations.

Interested readers can find various ERA40 seasonal and annual average fields depicted in an atlas published by ECMWF (Kållberg et al., 2005). Interested readers can presently create plots of NDRa2 data online at NCEP websites such as: http://www.cdc.noaa.gov/cdc/data.ncep.reanalysis2.html. However, very few fields can be directly compared (e.g. no zonal averages) using the ERA40 atlas and NDRa2 websites. A second purpose of this article is to make such comparisons for fundamental general circulation variables.

To compress the presentation, only DJF (December, January, and February average) and JJA (June, July, and August average) results are shown. The months used are drawn from the years 1979 – 2000 inclusive. All fields described are time averages where the two datasets overlap in time using the same naming convention. (NDRa2 variables change name after 2000.) Many variables are also averaged over longitude, such zonal averaging is indicated by using square brackets around the variable name. The multilevel data is provided on 2.5 by 2.5 latitude-longitude grid for both datasets. ERA40 single level fields use the same resolution. NDRa2 single level fields were provided on a 94 by 192 Gaussian grid that was regridded using NCL to the same 73 by 144 equally-spaced grid as the other data. Vertical levels present in both reanalyses are: 10, 20, 30, 50, 70, 100, 150, 200, 250, 300, 400, 500, 600, 700, 850, 925, and 1000 hPa.

Some fields don't have a precise match between datasets (such as radiation and cloud fields) which limits the scope of the comparisons here. Even so, datasets are used as available on line and as would be relevant to general circulation studies. Instructors preparing course materials, students doing homework, even researchers who do not have connections with those who prepared the data will limit their attention to what is available on line. So limited is the focus of this study.

2. Comparisons

2.1. Radiative fields (TOAswrf, TOAlwrf, sswrf, slwrf)

In studying the general circulation, the radiation fields are of primary importance since the uneven distribution of absorbed solar radiation is the ultimate driving force behind the general circulation. However, the radiation fields in the datasets may not be adequate for studying the general circulation. Trenberth (personal communication) says they are insufficient, since these fields are dominated by clouds which are not simulated well enough by the models used to generate the analyses. Allan et al. (2004) make a much more extensive comparison (than here) between ERA40, NNRa1, and satellite measurements of various radiative properties.

Further limiting our comparison of radiative fields is the issue that different types of radiation fields are provided in the available datasets. However, downward short wave and long wave radiation at the Earth's surface and top of atmosphere (TOA) are available for comparison in both datasets.

Net downward shortwave radiative flux at the top of the atmosphere (TOAswrf) indicates the solar radiative input into the earth-ocean-atmosphere system. TOAswrf is obviously larger in the summer hemisphere due to the tilt of the Earth's axis. On a global average, TOAswrf is slightly larger in ERA40 than NDRa2 Global means during DJF: 240.31 in NDRa2 and 243.00 in ERA40; during JJA: 230.63 in NDRa2 and 231.44 in ERA40. (The global means were calculated with a NCL-supplied zonal averaging and simple trapezoidal rule with cosine latitude weighting in latitude.) [TOAswrf] (Fig. 1) is systematically larger in the summer polar region by > 20 W m^{-2}. (The symbols: [ ] are used in this paper to indicate zonal average.) There is also some tendency for ERA40 data to be lower in the summer hemisphere middle latitudes, by ~10 W m^{-2}. Close to the equator, the ERA40 data tend to be larger by 10-25 W m^{-2} depending on the season. Geographically, the primary contributors to the higher equatorial values in ERA40 are the eastern Pacific and the Atlantic Ocean regions. Some of the difference field in the eastern Pacific is dipolar and consistent with the ICZ (judged from vertical motion, see below) being much narrower and further North there in ERA40 data. The Atlantic TOAswrf difference also reflects a narrower ICZ in ERA40 data. The high latitude summer difference seems linked to snow covered regions; during JJA the larger difference between datasets is over Greenland, with opposite sign to the difference over ice-free Siberia and North America. During DJF the TOAswrf is less (by 20-40 W m^{-2}) over the South Pacific Convergence Zone (SPCZ) which is more strongly defined (e.g. with higher estimated total cloud cover) in ERA40 data. The equatorial side of the summer subtropical highs has greater TOAswrf in ERA40 data, again total cloud cover is consistent in being estimated to be less there in ERA40 data.

Zonal mean net upward longwave radiative flux at the top of the atmosphere, [TOAlwrf] tends to be 2-5% larger in ERA40 over the winter midlatitudes. See Fig. 2. Near the equator, on the summer side, ERA40 is less by as much as 15 W m^{-2} though the two datasets agree better right at the equator. For shortwave and longwave radiation near the equator the TOA curves have more prominent ‘dips’ or ‘bumps’ in the ERA40 data; the primary reason for this difference is the ICZ has narrower meridional extent in ERA40 data over the Atlantic and the eastern Pacific. Where both datasets have an ICZ, they agree well in zonal mean data, where NDRa2 has a wider ICZ, they have larger disagreement. As with TOAswrf, the longwave flux in the region of the SPCZ is less in ERA40; a result that would be consistent with estimated greater high cloudiness (not shown) there in ERA40. Over nearly all of the Southern Hemisphere middle latitudes, ERA40 has slightly higher TOAlwrf (and lower TOAswrf). In the tropical, northwestern Pacific and to a lesser extent the Indian ocean ICZ, ERA40 has much smaller TOAlwrf (and smaller TOAswrf) in both seasons, but especially in summer (JJA), consistent with estimated total cloud cover (not shown) being greater there in ERA40 data. The differences over the Indian and west Pacific ICZ exceed 30 W m^{-2} over a large area; the disagreement exceeds 25%(!) in the South China Sea during JJA and Timor Sea during DJF. Outgoing longwave radiation (OLR) in this region is discussed in detail by Neuman et al. (2000; DJF); comparing ERA15 with NNRa1 and other data, some areas ERA15 performs better, some areas NNRa1 perform better. Speculating about the ERA40 versus NDRa2 differences seen here, perhaps there are more high clouds or colder cloud tops over the South China Sea and Timor Sea in NDRa2 data. Elsewhere in winter, major ice fields (Antarctica and Greenland) have smaller TOAlwrf in ERA40 whereas the north Atlantic, Barents Sea, and most of Russia have larger TOAlwrf in ERA40.

Averaging TOAlwrf estimates the heat lost by the planet. Global means during DJF: 240.52 in NDRa2 and 242.71 in ERA40; during JJA: 245.88 in NDRa2 and 247.62 in ERA40. The longwave flux leaving the planet should agree with the net short wave flux absorbed by the planet if the planet is not heating or cooling in the net. The downward solar and upward terrestrial values agree to within 0.3 W m^{-2} during DJF, but it puzzles the author that during JJA, the upward exceeds the downward radiative flux in both datasets by ~15 W m^{-2} suggesting net cooling during JJA. The scheme used for calculating the global mean is not exact, but would not be expected to have an error as large as 15 W m^{-2}.

Surface solar radiative flux (sswrf) downwards is more similar in the winter hemisphere than in the summer hemisphere, Fig. 3. On a zonal mean, ERA40 values tend to be lower in the winter middle latitudes (by roughly 5-20 W/m^2). In the higher latitudes during summer, ERA40 data is generally much less than NDRa2 data. For example, differences between datasets range from 30 W/m^2 at 40N to 100 W/m^2 (!) at the North Pole during JJA. ERA40 [sswrf] is similarly lower over much of Antarctica and adjacent

Ocean during DJF, except near the South Pole. The ICZ (intertropical convergence zone) is more narrowly defined (by a minimum in [sswrf]) which is also a little north of the corresponding minimum in NDRa2 data. Geographically, stronger differences occur over the Sahara and Arabian deserts, with ERA40 being larger by >20 W/m^2 over much of those deserts. Over the high elevations of Tibet, Rockies, and Andes, NDRa2 is larger by typically 40-80 W/m^2 with isolated points exceeding 150 W/m^2 difference, with the larger differences occuring in summer. Also in summer, NDRa2 data is larger over the subtropical oceans. The differences in handling the ICZ are most apparent over the tropical oceans. ERA40 is larger by >40 W/m^2 in the Eastern Pacific (DJF and JJA), across the Atlantic (mainly JJA). Some of the difference follows from NDRa2 having a latitudinally broader area of cloudiness in the Atlantic ICZ in JJA (also for the east Pacific ICZ in DJF). In the Indian Ocean the reanalyses are more similar though NDRa2 is larger along much of the ICZ. The global mean values of sswrf in DJF are 190.88 for NDRa2 and 185.08 for ERA40; and in JJA the global means are 179.88 and 169.14, respectively.

Surface thermal radiative flux (slwrf) downwards is quite similar in both datasets; see Fig. 4. On a zonal mean, ERA40 [slwrf] values tend to be larger (by 5-10 W/m^2) than NDRa2 values in middle latitudes. NDRa2 tends to have higher [slwrf] values for the subtropical region of sinking motion associated with the winter Hadley cell; a result of higher values over the oceanic regions, which are very uniformly higher (by >10 $W\ m^{-2}$) in NDRa2 data. ERA40 [slwrf] values are considerably higher in the summer polar region (12-16 W/m^2 during DJF over Antarctica; 20-45 W/m^2 over the Arctic in JJA). Geographically, the largest differences are found over mountainous regions, in particular: the Andes, Rockies, and Himalayas where ERA40 is larger (>90 W/m^2 at some grid points!). Generally, ERA40 has larger values (~20 W/m^2) over much of the Sahara and Europe. The global mean values of slwrf in DJF are 332.64 for NDRa2 and 335.50 for ERA40; and in JJA the global means are 348.57 and 352.66, respectively.

2.2. Temperature (T)

Zonal mean temperature in the middle to lower troposphere, between 30S and 90N, is similar in both reanalyses; [T] differences seen in Fig. 5 are generally less than 1 K. Near the tropical tropopause, [T] in ERA40 is ~3 K colder than NDRa2. (The peak difference occurs near 100 hPa and is spread over 20-40 degrees of latitude.) In the stratosphere above (20-50 hPa) NDRa2 is colder by ~1 K. In Southern Hemisphere midlatitudes, [T] is colder in ERA40 by ~1 K, especially in the lower and upper troposphere in both seasons. Over Antarctica, [T] below 500 hPa is warmer in ERA40 (up to 3.5 K, though the highest values are bogus, being for pressure levels that are "underground"), while in the upper troposphere (150-400 hPa) ERA40 is colder (up to 3.5 K) than NDRa2. The difference is roughly twice as large during summer and has a clear impact upon sea level pressure, as might be expected. In the ocean areas adjacent to Antarctica, lower tropospheric [T] is warmer by a degree or so in NDRa2. Geographically, the difference in T at 150 hPa is greatest over Antarctica, above the southern subtropical oceans all year, and the northern subtropical oceans in summer. In the tropics, T at 150 hPa has largest difference in the eastern Pacific and across the Atlantic oceans. Near the Earth's surface, T at 925 is about a degree warmer in NDRa2 over nearly all the oceans, somewhat consist with slwrf results shown above. Over much of Africa, ERA40 is warmer, by >2 K over most of the Sahara (DJF and JJA) and southern Africa (especially winter, by >2K). Generally, areas with higher elevation (n.b. some of these have surface pressure less than 925 hPa) are warmer in ERA40.

Trenberth et al. (2001, their Fig. 5) compare ERA15 and NNRa1 zonal mean temperatures and find ECMWF data to be cooler than NCEP data by more than 2 K near the tropical tropopause; that difference is reported as robust during sub-periods and appears quite similar to the difference reported here with ERA40 and NDRa2 data. They also find ERA15 data cooler (by 1 K) in lower troposphere of the Southern Hemisphere midlatitudes, again this difference continues with the longer, more recent data compared here. Simmons et al. (2004) remark that the ERA40 data in the time period studied here has a cold bias by roughly a degree in the Southern Hemisphere middle latitudes, but in the mid troposphere.

2.3. Mass fields (slp, Z)

Sea level pressure (slp, not shown) has similar zonal mean in the two models north of 65S. Zonal mean differences are generally less than 1 hPa except in polar regions. North of 55N during DJF, [slp] differences approach 2 hPa at the North Pole. South of 65S, [slp] is much lower (by up to 12 hPa) in ERA40. The [slp] differences are greater during summer, as was [T]. [slp] over topography is extrapolated from surface pressure using an exponential. The exponential argument is inversely related to surface temperature so the extrapolation from surface pressure is greater in NDRa2 (since it is colder) than in ERA40, consequently, NDRa2 has higher [slp]. Geographically, the only noteworthy differences are associated with topographic features. ERA40 slp is much less (>20 hPa) over much of Antarctica, and less (by >6 hPa) over the Tibetan plateau, during winter. The global mean slp during DJF is 1011.43 hPa in NDRa2 and 1011.45 hPa in ERA40; during JJA the corresponding means are 1011.45 and 1011.20. Trenberth and Smith (2005) have compared a different quantity, *surface* pressure, and found larger differences between NNRa1, ERA40, and ERA15 than found for global mean *sea level* pressure here; they find global mean surface pressure was ~0.3 hPa greater in ERA40, than NNRa1. Unfortunately, surface pressure is not in the online ERA40 products supplied by ECMWF.

Geopotential height (Z, not shown) responds predictably to the T differences in the datasets. [Z] throughout the middle and lower troposphere (>400 hPa) north of 50S has less than 10m difference between the datasets. Over Antarctica, the colder temperatures of the NDRa2 reanalysis lead to lower heights; the difference in [Z] is about 20 m at levels between 300 and 500 hPa over Antarctica. In the tropical lower stratosphere, ERA40 [Z] heights are lower (by ~90 m in DJF, by ~50 m in JJA); this difference reflects the lower tropical tropopause temperatures mentioned above. Geographically, the largest differences in Z at 150 hPa are above: Antarctica, the Southern Hemisphere oceans, and the northern oceans (mainly JJA). The smallest differences (<20 m) tend to occur over Australia, and landmasses north of 20N.

2.4. Velocity fields (U, V, ω, meridional circulation)

Zonal mean zonal wind [U] is similar in both analyses through much of the troposphere as might be anticipated from the similar [Z] fields (geostrophic wind considerations). The Southern Hemisphere subtropical jet is stronger in ERA40 by 1-2 m/s. See Fig. 6. However, an intriguing difference is found in the tropical upper troposphere during DJF. The difference in [U] between 100 to 200 hPa and 10S to 5N is about 2 m/s. This seemingly small difference is sufficient to reverse the sign of [U] in that region; weak westerlies occur in ERA40 and weak easterlies occur in NDRa2. During JJA, both datsets have tropical easterlies through the depth of the troposphere, though the westerlies extend deeper into the tropics in the Southern Hemisphere levels near the tropopause in ERA40. In the lower stratospheric subtropics, ERA40 data has stronger [U] easterlies (by several m/s) than the NDRa2 reanalysis.

Geographically, during DJF both datasets have westerlies at 150 hPa over the eastern Pacific and central Atlantic; in ERA40 these westerlies are 4-9 m/s more westerly. (See upper panel, Fig. 7) The region of westerlies is similar in the east Pacific but is broader (longitudinally) in the Atlantic (near 20S). Dynamical theory (Webster and Holton, 1982; Branstator, 1983) suggests that tropical easterlies will reflect energy approaching the equator whereas westerlies would allow such information (apparent as a stationary wavetrain) to propagate into the opposite hemisphere. Theory predicts that the stronger the westerlies, the easier the interhemispheric propagation, so the datasets appear to allow different interhemispheric communication. Easterlies in ERA40 are also several m/s slower over the Indian Ocean during DJF.

During JJA, equatorial easterlies are stronger by several m/s in ERA40 over the eastern Pacific and western Atlantic (e.g. 150 hPa level; lower panel, Fig. 7). One consequence is the longitudinal range of tropical westerlies over northern South America is wider in NDRa2 than in ERA40 (somewhat contrary to the DJF result).

Meridional motions on the zonal mean, [V, not shown] emphasize the winter hemisphere Hadley circulation. The upper tropospheric "return flow" of the winter hemisphere Hadley cell in ERA40 has stronger peak value (3.5 m/s in NDRa2 versus 4 m/s in ERA40) and extends through a greater depth (higher and lower) during DJF. During JJA, the ERA40 return flow is again stronger (by ~0.5 m/s) and a bit deeper. Geographically, the JJA return flow has larger differences between datasets along a band extending across the equatorial Indian ocean to the eastern Pacific; V is stronger, by >1.5 m/s, in NDRa2 data. However, the return flow over the subtropical Atlantic and southern Africa is a bit weaker in NDRa2 JJA data. In DJF, the prime contributors to the stronger ERA40 return flow are over the Sahara, and along a band from the northeastern Indian ocean across most of the equatorial Pacific.

Zonal mean pressure velocity [ω] has a single large maximum in NDRa2 DJF data but two distinct maxima in ERA40 DJF data (Fig. 8). That second maximum causes [ω] in ERA40 to differ by about half the magnitude of the primary maximum. The secondary maximum found only in ERA40 DJF [ω] is centered near 5N. Geographically, the source of the secondary maximum is the ICZ over the eastern Pacific and central Atlantic; the ICZ in those regions is much stronger and meridionally narrower in ERA40 data (Fig. 9). In fact, NDRa2 ω data has *sinking* where one might expect rising for an Atlantic ICZ during DJF. Over the Indian Ocean and consistent with [V] data, the rising motion is broader and more zonally-varying in NDRa2 data. During JJA, the NDRa2 data recover an Atlantic ICZ, though it is broader and weaker than in ERA40. Even though the grid points are the same, the NDRa2 ω field is noticeably smoother than the same field in ERA40 data. JJA ERA40 data have a 'wavier' ω field near major steep-sloped topographic features such as the Andes, Rockies, and Himalayas.

The changes to vertical and meridional motions show up in somewhat coherent difference fields of the zonal mean meridional circulation. Fig. 10 shows arrows depicting the mean meridional cells. The winter Hadley circulation is the most prominent feature. Also shown is the 'difference circulation' composed of the difference between ERA40 and NDRa2 fields of [V] and [ω]. In the DJF difference circulation has some indication of the missing or weaker Atlantic and eastern Pacific winter Hadley cell in NDRa2 data. In JJA data the difference circulation again shows some evidence for a weaker winter Hadley cell in NDRa2 data. Close inspection finds that some low level arrows of the difference circulation oppose each other, most notably in the DJF panel; a result that reflects the stronger ICZ in ERA40 in the eastern Pacific, a portion of the ICZ that has less seasonal migration than elsewhere along the ICZ.

2.5. Moisture (q, total cloud cover, P)

Specific humidity (q) is provided in the ERA40 data but must be created from T and relative humidity at isobaric levels in the NDRa2 data. Specific humidity (Fig. 11) is largest in the tropical lowest levels, decreasing rapidly towards the poles and with increasing elevation. The zonal average, [q] has greatest magnitude difference between the datasets in the tropical lower half of the troposphere. Generally, [q] is much larger (ranging from 5-25%) in ERA40 data where there is rising motion of the Hadley cells. In lower half of the troposphere in the adjacent subtropics, [q] is less (by 5-20%) in ERA40. The difference (ERA40 minus NDRa2) is positive from 20S to 10N during DJF and from equator to 30N during JJA for pressure greater than 300 hPa. During DJF, the geographic distribution of the difference at the representative level, 700 hPa is as follows. ERA40 has greater q in the Atlantic ICZ across equatorial Africa; ERA40 is ~15% larger along the ICZ across the southern Indian ocean into the western Pacific; ERA40 is also wetter (by ~50%) in the south Pacific convergence zone (SPCZ). In the eastern Pacific, south of the equator, ERA40 is generally drier by up to 50%. During JJA, the difference at 700 hPa is as follows. The difference is positive over most of the northern tropical oceans, especially the western Pacific and New Guinea, where ERA40 is up to a third larger than NDRa2. The SPCZ is narrower in ERA40 leading to larger negative differences in the South Pacific. Generally south of the ICZ NDRa2 has more water vapor, in the central south Pacific results from the wider SPCZ mentioned. In the south Indian Ocean, the dipolar difference results from topical NDRa2 having less peak moisture (at the equator) but extending further south before having a sharp meridional gradient. Trenberth et al.

(2001) also find higher specific humidity values in ERA40 data in the lower half of the tropical troposphere compared with NNRa1.

The total cloud cover is expressed as a percent fraction of the sky. Total cloud cover is provided in ERA40 whereas the NDRa2 data have total cloud cover at various levels or ranges of levels. Hence it is not possible to directly compare the datasets. One cannot determine either variable from the other without making assumptions. As a rough comparison, it is assumed that the total cloud cover equals the fraction of high cloud cover plus the fraction of clear sky at high level multiplying the fraction of cloud cover at middle level, plus the remaining fraction of clear sky multiplying the fraction of lower level cloud. When estimated this way, the NDRa2 data are similar in range to the ERA40 data: matching well for the ICZ maximum and summer subtropical minimum, ERA40 being cloudier in the winter subtropics and year around in polar regions. Again, these comparisons are not precise.

Frequent mention has been made here of ERA40 data having narrower ICZ in the Atlantic and eastern Pacific. Cloud climatologies from satellite data (e.g. Miller and Feddes, 1971; see also Grotjahn, 1993, plate 2 and fig. 5.13) show quite a narrow time mean ICZ-related cloudband across the eastern Pacific and a less narrow cloud band across the Atlantic. Such cloud climatologies seem more comparable to the ERA40 depiction. A comparison of ERA40 and ISCCP decadal time mean (Allan et al., 2004) shows agreement to within 10% over the Atlantic and eastern Pacific, with ERA40 being roughly 10% too cloudy in the western Pacific..

Precipitation rate (P) is presented here as mm per day and has largest maximum along the tropical ICZ. See Fig. 12. Secondary maxima occur in middle latitudes associated with frontal cyclone storm tracks. During DJF, [P] has a double maximum in the tropics in ERA40 data but a single maximum in NDRa2 data; this result is consistent with the vertical motion field in Fig. 8. Geographically, the DJF difference shows that ERA40 has much larger P (often by 50 - 100%) along the Atlantic and eastern Pacific ICZ, again as might be anticipated from greater upward motion there in the ERA40 data.

The subtropical minimum is a bit lower in ERA40 in both hemispheres and both seasons. The middle latitude secondary maximum is generally larger for NDRa2 data for the Northern Hemisphere during both DJF and JJA. In the Southern Hemisphere during JJA the midlatitude maximum is about the same during DJF, but during JJA NDRa2 [P] is again larger. Geographically, JJA precipitation rate along the eastern Pacific ICZ is again stronger in ERA40 data over the oceans. In contrast to DJF, precipitation rate along the Atlantic ICZ is stronger in NDRa2 data. NDRa2 is also locally much larger (by up to 100% more) over southern India and southeast Asia. As Neuman et al. (2000) noticed for the precursor datasets ERA15 and NNRa1, both ERA40 and NDRa2 have a ‘double’ ICZ across the western half of the Pacific (from roughly 160W to 120E) in DJF. In JJA ERA40 has a double ICZ of similar extent, but NDRa2 does not owing to a stronger northern branch of ICZ in the west Pacific ‘warm pool’. Also, while the island of New Guinea has more P in ERA40, the Pacific Ocean to the north has less P in ERA40 than NDRa2. The greater New Guinea P may reflect different topographic formulations in the models used by the two datasets. In the Northern Hemisphere midlatitudes, NDRa2 data are larger over the oceanic storm tracks during DJF; but during JJA, NDRa2 data are larger mainly over land areas, specifically: northwestern Canada, southeastern United States, eastern Europe, and northwestern Russia. The global average P in DJF is 3.03 in NDRa2 and 3.12 in ERA40; in JJA the global means are 3.28 and 3.12, respectively.

Other studies have compared P in the precursor datasets. In the Arctic, Serreze and Hurst (2000) are critical of NNRa1 P data while concluding that ERA15 data are superior. In the Asian monsoon region Annamalai et al. (1999) compare NNRa1 and (essentially) ERA15 data over the 1979-1995 period. They conclude that the ECMWF data is superior. Comparing the same time period (not shown) some aspects of P in NDRa2 have improved noticeably over NNRa1, though other aspects may be less well. NDRa2 matches observational datasets of Legates and Willmott (1990) and Xie and Arkin (1996) better than did NNRa1 at the SW coast of India and the Myanmar coast; previously NNRa1 P was much too weak, now NDRa2 P may be a bit too strong. In the western Pacific those observational datasets seem better matched in some regions (north of New Guinea) by NDRa2 than ERA40 during that time period; in other areas ERA40 looks comparable or qualitatively better. Over the Himalayas, NDRa2 has less P than NNRa1 becoming perhaps too little compared to those observational datasets, while ERA40 is much larger than the observational datasets.

2.6. Energetics (SHF, LHF, MSE, KE)

Surface sensible heat flux (SHF, Fig. 13) is available in both datasets. Surface sensible heat flux plays a role in exchange of energy between the atmosphere and the earth's surface. In both datasets, SHF is positive over oceans in the tropics and most of the middle latitudes of the winter hemisphere. Near the western boundary currents in winter, SHF is large in both datasets, but is 20-50% larger in NDRa2. Over North America and Eurasia in DJF, SHF is negative and more strongly so in NDRa2 data. In contrast, during JJA, the Northern Hemisphere continents have positive SHF which is more similar in the two datasets. ERA40 tends to have larger positive SHF over the oceans (except Arctic) in JJA, too. SHF is negative over most of the Arctic, and perhaps more strongly so in NDRa2 data. These geographic variations cause [SHF] to be systematically larger in ERA40 data. The difference in [SHF] between datasets tends to increase towards higher latitudes, exceeding 10 W/m^2 in polar regions. The global mean of SHF in DJF is 6.06 in NDRa2 and 14.00 in ERA40; in JJA the global means are 10.05 and 16.99, respectively.

Another component of the surface energy budget is surface latent heat flux (LHF, Fig. 13). Unlike [SHF], [LHF] is positive for all latitudes in both datasets. [LHF] is also often much larger than [SHF]. Both datasets have relative maxima of [LHF] in the subtropics. The two maxima are similar in DJF; in JJA the Southern Hemisphere max is about 20% larger. The fluxes generally decrease towards the poles, with a weak secondary maximum at high northern latitudes. The [LHF] is systematically less in ERA40 data for most latitudes north of 30S. Differences in [LHF] range around 5-20 W/m^2 at many latitudes. Recall that the corresponding [SHF] difference had opposite sign in these latitudes. The two datasets have quite similar [LHF] in latitudes south of 30S. The global mean of LHF in DJF is 88.86 in NDRa2 and 81.55 in ERA40; in JJA the global means are 93.27 and 84.91, respectively. Geographically, NDRa2 data is larger than ERA40 data over nearly all of the tropics, both ocean and continental areas. The difference is largest where the field is larger, such as the non-ICZ portion of the tropical Atlantic (during JJA: 5N to 20N and 10S to 15S where differences exceed 40 W m^{-2}).

For tropical and some subtropical latitudes moist static energy (MSE) decreases with increasing elevation in the lowest 200-300 hPa due to the rapid decline of specific humidity as elevation increases. Elsewhere in the troposphere, MSE increases with elevation due to the statically stable nature of the atmosphere. Given its higher static stability, MSE increases even more rapidly with increasing elevation in the stratosphere. MSE change with elevation is crucial for a mass-conserving circulation like the Hadley cell to have a net transport of heat. To transport heat poleward, the upper branch of the Hadley cell must be in air of higher MSE than the equatorward flow underneath. In the tropics and low subtropics, this net vertical difference in heat transport is much smaller (by a couple orders of magnitude) than each of the opposing heat transports. It is shown above that the ERA40 data have higher q (specific humidity) in the lower troposphere and lower temperature in the upper troposphere; this combination means that the difference in MSE between upper and lower troposphere is less in the ERA40 data than in NDRa2 data. It is also shown above that the ERA40 data have a stronger Hadley circulation. Hence, compared to the NDRa2 heat transport, ERA40 data have a faster circulation that could be compensating for a smaller vertical difference in MSE. These properties of [MSE] are seen in Fig. 14.

Calculation of the net meridional heat flux is a vertical integral that is not easily made precise from the supplied data. The vertical integral from 1000 to 10 hPa of [V] should be nearly zero, except for interhemispheric mass transfers. Using a crude trapezoidal rule approximation to that integral yields vertical mean [V] at 5N during DJF of: 3 mm/s in NDRa2 and 41 mm/s in ERA40; the corresponding values at the equator in JJA are: -21 mm/s in NDRa2 and -64 mm/s in ERA40. These estimates are too crude to trust fully corresponding net heat flux calculations. With that caveat, the corresponding net heat fluxes are similarly different: ERA40 values of the net heat flux tend to exceed the NDRa2 values when calculated this way. For the indicated latitudes and seasons, the net heat flux is 2-3 times as large. The tropical tropopause is near the data level 100 hPa. If the integration range in pressure is restricted to 100 to 1000 hPa, the net vertically integrated meridional velocity and MSE flux are even worse, with DJF NDRa2 values having incorrect sign for MSE flux. Clearly these results are discouraging and use of either dataset to deduce net heat fluxes requires caution and more care. The interested reader is directed to Trenberth et al. (2002) for a much more thorough discussion of how to properly calculate vertical integrals from data interpolated to isobaric levels.

Kinetic energy (KE, Fig. 15) is larger in ERA40 data than in NDRa2 data. As noted above, the [U] subtropical jet stream is stronger in ERA40 data, especially in the Southern Hemisphere during winter. In the Northern Hemisphere the difference is larger again during winter. The stratospheric polar night (winter) jet is stronger and wider in ERA40 data during DJF making the KE about 1/3 larger and extending further poleward, leading to the larger differences; in JJA, the [KE] magnitudes are similar between datasets, but the ERA40 data again extends further poleward, leading to large differences. Finally, the datasets differ in the stratospheric equatorial [KE], which is more than twice as large in ERA40 data. Geographically, the differences mirror differences seen in zonal wind. At 200 hPa and during DJF, ERA40 has higher KE over the southern ocean subtropical jet (>100 m^2 s^{-2}), the southeastern tropical Pacific (>140 m^2 s^{-2}), northern hemisphere subtropical jet (> 140 m^2 s^{-2}) over the western Pacific with peak differences closer to 120 m^2 s^{-2} over Asia and northern Africa. At 200 hPa and during JJA, ERA40 data are again stronger over the subtropical jets of the south Pacific (> 175 m^2 s^{-2}) and south Indian (>250 m^2 s^{-2}) Oceans, the Northern Hemisphere jet is stronger (>100 m^2 s^{-2}) only east of Japan. As noted above, NDRa2 has a stronger JJA tropical Indian ocean easterly jet, so NDRa2 KE is larger (>100 m^2 s^{-2}) there.

3. Conclusions

In recent years a huge effort has been made at operational centers in the U.S. and ECMWF to make available internally consistent, long term stable collections of gridded atmospheric data. Two important, recent datasets, here labeled NDRa2 and ERA40 have been compared. It is beyond the scope of this article to assess which dataset is “more correct” and the author is loath to do so given the great value of each dataset and the great effort expended to produce and make easily available both datasets. Earlier ‘precursor’ versions of the datasets have been compared by others, though for a more limited region or set of variables. For example, Bromwich and Wang (2005) compare ERA15, ERA40, and NNRa1 data over the Arctic against selected radiosonde stations and conclude that ERA40 capture better properties seen in the observations.

The datasets disagree in some global mean radiative properties, but those who study radiation probably would seek out other sources, such as working with satellite data directly. Many of the differences quantified here agree qualitatively with comparisons of the precursor datasets (ERA15 and NNRa1) made by others and those are noted above.

Zonal mean differences are often associated with lower tropical upper troposphere temperatures in ERA40. The zonal mean zonal winds tend to be stronger (especially the jets) in ERA40 data which also boosts the kinetic energy. The winter Hadley cell is stronger and has more complexity in ERA40 data.

The solar and infrared radiation are similar in the tropical regions; where they differ is mainly showing a tendency for the rising in the ICZ to be narrower focused and stronger in ERA40 data. However, at the surface ERA40 has more heat entering the atmosphere in sensible form, whereas NDRa2 data have more entering as latent heat. Consequently, specific humidity, q tends to be larger in NDRa2 data in the subtropics. But since the veritical motion is stronger and maybe more narrowly focused in latitude, ERA40 has higher q values carried into the middle troposphere close to the equator, with NDRa2 data larger further afield. In the end, the horizontal tropical rainfall is quite similar, except for ERA40 greater precipitation contributed in the tropical Atlantic and eastern Pacific.

The datasets have some geographic regions where they disagree in many different variables. One of the most significant regions of difference is the treatment of the equatorial regions of the Atlantic and eastern Pacific; for example, the ICZ is more sharply defined and its vertical circulation appears stronger in ERA40 data. Topography seems to create other locally large differences, especially the Tibetan Plateau, the Andes, Greenland, and nearly all of Antarctica.

To answer the question posed by the title of this article, the different datasets do give notably different general circulations, especially in the tropics. The difference is not easily summarized as one dataset having a stronger Hadley cell than the other, since ERA40 is strong in some regions (Atlantic and east Pacific) while NDRa2 is stronger in others (Indian and west Pacific). The models differ in their dynamics, with stronger (subtropical and polar night) jetstream winds in the ERA40 data. ERA40 has equatorial upper tropospheric westerlies where easterlies prevail in NDRa2 and that may allow more communication between hemispheres in ERA40's general circulation.

Acknowledgments

ECMWF ERA-40 (ERA40) data used in this study have been obtained from the ECMWF data server. The NCEP/DOE AMIP-II Reanalysis (NDRa2) data used in this study have been obtained from the NOAA, National Weather Service, Climate Prediction Center data server. The author greatly appreciates related email correspondence from Drs. Grant Branstator, Kevin Trenberth, and Wesley Ebisuzaki. This material is based upon work supported by the National Science Foundation under Grant No. ATM- 0354545.

References:

Allan, R. P., Ringer, M.A., Pamment, J.A., Slingo, A., 2004. Simulation of the Earth's radiation budget by the European Centre for Medium-Range Weather Forecasts 40-year reanalysis (ERA40), J. Geophys. Res., 109, D18107, doi:10.1029/2004JD004816.

Annamalai, H., Slingo, J.M., Sperber, K.R., Hodges, K., 1999. The Mean Evolution and Variability of the Asian Summer Monsoon: Comparison of ECMWF and NCEP–NCAR Reanalyses. *Mon. Wea. Rev.* **127**, 1157–1186.

Branstator, G., 1983, Horizontal energy propagation in a barotropic atmosphere with meridional and zonal structure. J. Atmos. Sci., 40, 1689-1708.

Bromwich, D.H., Wang, S-H., 2005. Evaluation of the NCEP–NCAR and ECMWF 15- and 40-Yr Reanalyses Using Rawinsonde Data from Two Independent Arctic Field Experiments. *Mon. Wea. Rev.* **133**, 3562–3578.

Grotjahn, R., 1993. *Global Atmospheric Circulations: Observations and Theories*. Oxford Univ. Press., New York, 430 pp.

Kållberg, P., Berrisford, P., Hoskins, B., Simmons, A., Uppala, S., Lamy-Thépaut, S., Hine, R., 2005. *ERA-40 Atlas*. ERA-40 Project Report Series No. 19, 191pp.

Kalnay, E. Kanamitsu, M. Kistler, R. Collins, W. Deaven, D. Gandin, L. Iredell, M. Saha, S. White, G. Woollen, J. Zhu, Y. Leetmaa, A. Reynolds, B. Chelliah, M. Ebisuzaki, W. Higgins, W. Janowiak, J. Mo, K.C. Ropelewski, C. Wang, J. Jenne, R., Joseph, D., 1996. The NCEP/NCAR 40-Year Reanalysis Project. *Bul. Amer. Meteor. Soc*. **77**, 437–471.

Kanamitsu, M., Ebisuzaki, W., Woollen, J., Yang, S-K., Hnilo, J., Fiorino, M., Potter, G., 2002. NCEP–DOE AMIP-II Reanalysis (R-2). *Bul. Amer. Meteor. Soc*. **83**, 1631–1643.

Kistler, R., Kalnay, E., Collins, W., Saha, S., White, G., Woollen, J., Chelliah, M., Ebisuzaki, W., Kanamitsu, M., Kousky, V., van den Dool, H., Jenne, R., Fiorino, M., 2001, The NCEP–NCAR 50–Year Reanalysis: Monthly Means CD–ROM and Documentation. *Bul. Amer. Meteor. Soc.*, **82**, 247–267.

Legates, D. R., Willmott, C.J., 1990: Mean, seasonal and spatial variability in gauge corrected global precipitation. *Int. J. Climatol.,* **10,** 111–127.

Miller, D.B., Feddes, R.G., 1971. "Global Atlas of Relative Cloud Cover." U.S. Nat'l Envr. Sat. Serv. And USAF Envr. Tech. Appl. Cntr., AD 739434 – Rep. No. 1, Washington, DC., 14 pp. plus charts.

Newman, M., Sardeshmukh, P.D., Bergman, J.W., 2000: An Assessment of the NCEP, NASA, and ECMWF Reanalyses over the Tropical West Pacific Warm Pool. *Bul. Amer. Meteor. Soc.*, **81**, 41–48.

Renwick, J. A., 2004. Trends in the Southern Hemisphere polar vortex in NCEP and ECMWF reanalyses, Geophys. Res. Lett., 31, L07209, doi:10.1029/2003GL019302.

Serreze, M.C., Ciaran M. Hurst, C.M.,. 2000. Representation of Mean Arctic Precipitation from NCEP–NCAR and ERA Reanalyses. *J. Climate*.**13**, 182–201.

Simmons, A. J.; Jones, P. D.; da Costa Bechtold, V.; Beljaars, A. C. M.; Kållberg, P. W.; Saarinen, S.; Uppala, S. M.; Viterbo, P.; Wedi, N. 2004. Comparison of trends and low-frequency variability in CRU, ERA-40, and NCEP/NCAR analyses of surface air temperature. *J. Geophys. Res.,* 109, D24115, doi:10.1029/2004JD005306.

Trenberth, K. E., Smith, L., 2005: The Mass of the Atmosphere: a Constraint on Global Analyses. *J. Climate*, **18**, 864-875.

Trenberth, K. E., Stepaniak, D. P. Caron, J. M., 2002: Accuracy of atmospheric energy budgets. *J. Climate*, **15**, 3343-3360.

Trenberth, K. E., Stepaniak, D. P., Hurrell, J. W., Fiorino, M., 2001: Quality of reanalyses in the tropics. *J. Climate*, **14**, 1499–1510.

Uppala, S.M., Kållberg, P.W., Simmons, A.J., Andrae, U., da Costa Bechtold, V., Fiorino, M., Gibson, J.K., Haseler, J., Hernandez, A., Kelly, G.A., Li, X., Onogi, K., Saarinen, S., Sokka, N., Allan, R.P., Andersson, E., Arpe, K., Balmaseda, M.A., Beljaars, A.C.M., van de Berg, L., Bidlot, J., Bormann, N., Caires, S., Chevallier, F., Dethof, A., Dragosavac, M., Fisher, M., Fuentes, M., Hagemann, S., Hólm, E., Hoskins, B.J., Isaksen, L., Janssen, P.A.E.M., Jenne, R., McNally, A.P., Mahfouf, J.-F., Morcrette, J.-J., Rayner, N.A., Saunders, R.W., Simon, P., Sterl, A., Trenberth, K.E., Untch, A., Vasiljevic, D., Viterbo, P., Woollen, J. 2005: The ERA-40 re-analysis. *Quart. J. R. Meteorol. Soc.*, **131**, 2961-3012.

Webster, P., Holton, J., 1982, Cross equatorial response to middle latitude forcing in a zonally varying basic state. *J. Atmos. Sci.*, **39**, 722-733.

Xie, P., Arkin, P., 1996. Analyses of global monthly precipitation using gauge observations, satellite estimates, and numerical model predictions. *J. Climate,* **9,** 840–858.

Figure Captions

Fig. 1. Net downward shortwave radiative flux at the top of the atmosphere during December-February (DJF, left column) and June-August (JJA, right column) for the 22 year period 1979-2000. (Net is downward minus upward reflected solar radiation.) Top row: solid line NDRa2 [TOAswrf] data, dashed line ERA40 data. Middle row: ERA40 minus NDRa2 [TOAswrf] difference. Bottom row: geographical distribution of the TOAswrf difference: ERA40 minus NDRa2 data with contour interval of 20; negative values shaded. Units are W m^{-2}. Notable differences occur near the ICZ and SPCZ and polar ice sheets of the summer hemisphere.

Fig. 2. Similar to fig. 1, except showing longwave upward radiative flux at the top of the atmosphere. Units are W m^{-2} and contour interval is 10 W m^{-2}. Large differences (up to 25%) occur near much of the ICZ and SPCZ.

Fig. 3. Similar to fig. 1, except showing short wave radiative flux reaching the surface. Units are W m^{-2} and contour interval is 20 W m^{-2}. Notable differences occur near the ICZ and SPCZ and high latitudes of the summer hemisphere.

Fig. 4. Similar to fig. 1, except showing surface longwave radiative flux. Units are W m^{-2} and contour interval is 10 W m^{-2}. Notable differences occur near higher topography and polar land areas. Winter subtropical oceans have uniformly larger slwrf in NDRa2 data.

Fig. 5. Zonal mean temperature, [T]. NDRa2 data top row, ERA40 data middle row, difference: ERA40 minus NDRa2 bottom row. Left column DJF, right column JJA. Contour interval is 10 K for top and middle row, 1 K for bottom row. Negative values (ERA40 cooler) are shaded. Tropical tropopause and lower level Southern Hemisphere midlatitudes are colder in ERA40 data.

Fig. 6. Similar to fig. 5 except showing zonal mean zonal wind, [U]. ERA40 has equatorial, upper tropospheric westerlies not seen in other datasets during DJF. Larger differences occur in the stratosphere, where ERA40 data often have stronger easterlies in

middle stratosphere, weaker near equatorial tropopause. Stratospheric winter polar night jet is stronger in ERA40 data. Contour interval is 5 m/s for top and middle row, 1 m/s for bottom row. Shaded areas indicate negative values (easterlies).

Fig. 7. Geographic distribution of zonal wind difference, ERA40 minus NDRa2 at 150 hPa for DJF (top) and JJA (bottom). Contour interval is 1 m/s. Shaded areas are where the difference is negative. Larger differences occur over the tropical Atlantic and eastern tropical Pacific. In DJF, NDRa2 data have stronger easterlies over Atlantic and across Indian oceans; in ERA40, region of westerlies is wider longitudinally in tropical Atlantic.

Fig. 8. Similar to the left column of fig. 5, except for zonal mean cross sections of pressure velocity ($\omega = dP/dt$). Contour interval is 0.01 Pa/s for top and middle plot, 0.005 for the difference field (bottom plot); shaded areas indicate negative values (upward motion). ERA40 has a "second" peak rising zone near 5 N in $[\omega]$ that is not apparent in NDRa2 data.

Fig. 9. Comparison plots of time mean pressure velocity ($\omega = dP/dt$) for NDRa2 data (top row) and ERA40 data (bottom row) during DJF (left column) and JJA (right column). Despite using the same grid, the NDRa2 data tend to have broader features such as parts of the ICZ. NDRa2 data have very weak ICZ in the central Atlantic and weaker ICZ in the east Pacific than ERA40 during DJF. The Atlantic and east Pacific ICZ is at a higher latitude than many other regions, consequently, ERA40 data have the 'second' peak rising zone mentioned in previous figure. Near steep-sloped topographic features, such as the Himalayas and the Andes ω has more waviness in ERA40 data. Contour interval is 0.03 Pa/s; shaded areas indicate negative values (upward motion).

Fig. 10. Similar to fig. 5 except using vectors to show the zonal mean circulation in the meridional and vertical plane.

Fig. 11. Zonal mean specific humidity [q] ERA40 data top row, [q] difference: ERA40 minus NDRa2 middle row, bottom row is difference in q, ERA40 minus NDRa2 at 700

hPa level. Left column DJF, right column JJA. Contour interval is 1 gm/kg for top and bottom rows, 0.2 gm/kg middle row. Negative values are shaded. Distribution of [q] for NDRa2 very similar in appearance to top row. ERA40 has higher q than NDRa2 along most of the ICZ, lower in much of the winter hemisphere subtropics.

Fig. 12. Similar to fig. 1 except showing precipitation rate, P. Units are mm/day and the contour interval is 2 mm/day. ICZ in Atlantic and eastern Pacific has greater P in ERA40. In contrast, NDRa2 data has larger ICZ-associated P in Indian and west Pacific oceans. During winter, P in midlatitude storm tracks is generally less in ERA40. During JJA, less P in ERA40 over northern continents.

Fig. 13. Zonal mean surface sensible heat flux, [SHF] and ERA40 minus NDRa2 difference (top and second row, respectively). Zonal mean surface latent heat flux, [LHF] and ERA40 minus NDRa2 difference (third and bottom row, respectively). In top and third rows: solid line is NDRa2; dashed line is ERA40. Units are W m^{-2}.

Fig. 14. Similar to fig. 5 except for zonal mean kinetic energy, [KE]. Contour interval is 200 $m^2 s^{-2}$ except for bottom row which uses interval 25 $m^2 s^{-2}$. ERA40 data generally have more [KE] especially in winter stratosphere, winter subtropical jet, and tropical stratosphere.

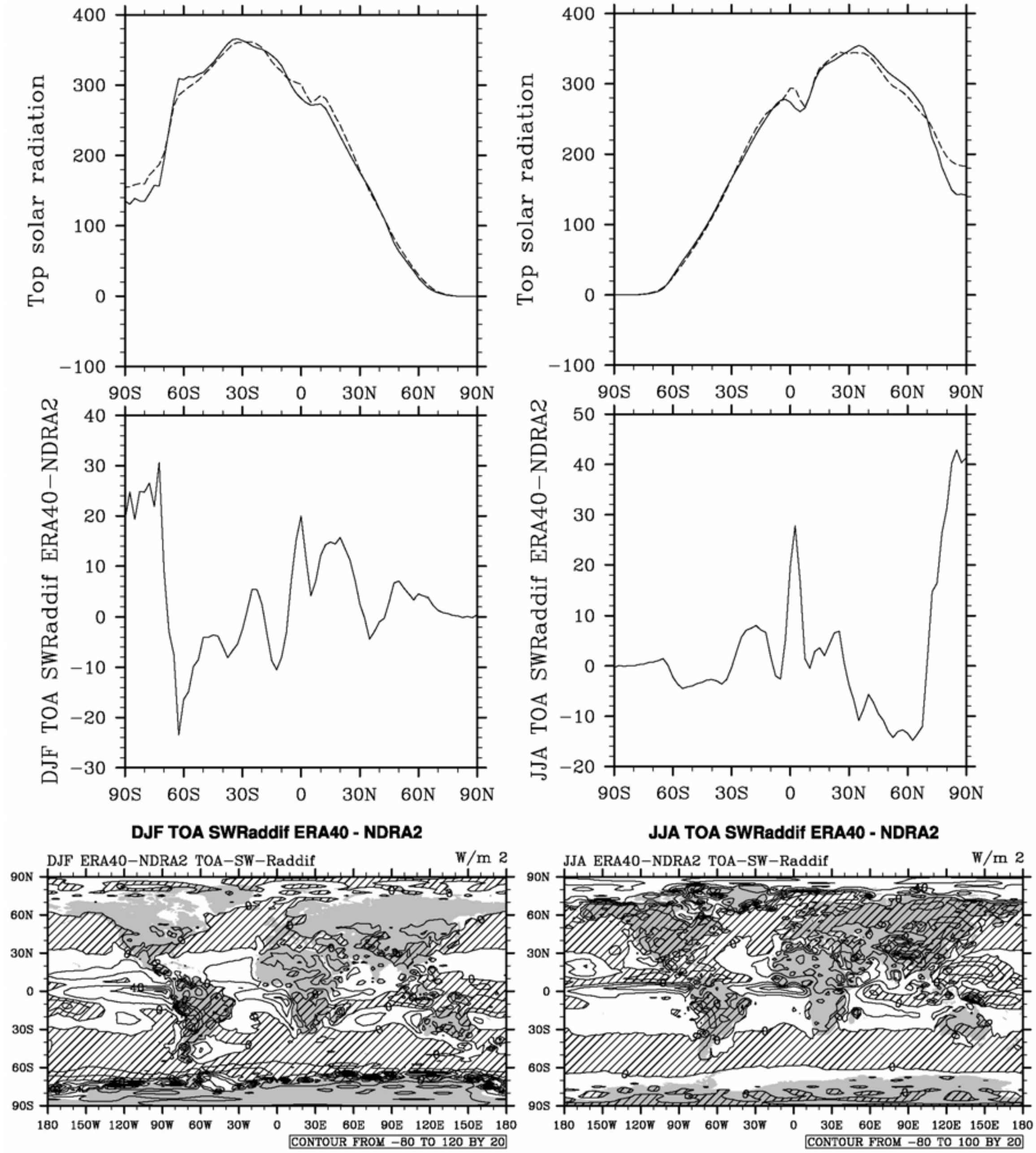

Fig. 1. Net downward shortwave radiative flux at the top of the atmosphere during December-February (DJF, left column) and June-August (JJA, right column) for the 22 year period 1979-2000. (Net is downward minus upward reflected solar radiation.) Top row: solid line NDRa2 [TOAswrf] data, dashed line ERA40 data. Middle row: ERA40 minus NDRa2 [TOAswrf] difference. Bottom row: geographical distribution of the TOAswrf difference: ERA40 minus NDRa2 data with contour interval of 20; negative values shaded. Units are W m^{-2}. Notable differences occur near the ICZ and SPCZ and polar ice sheets of the summer hemisphere.

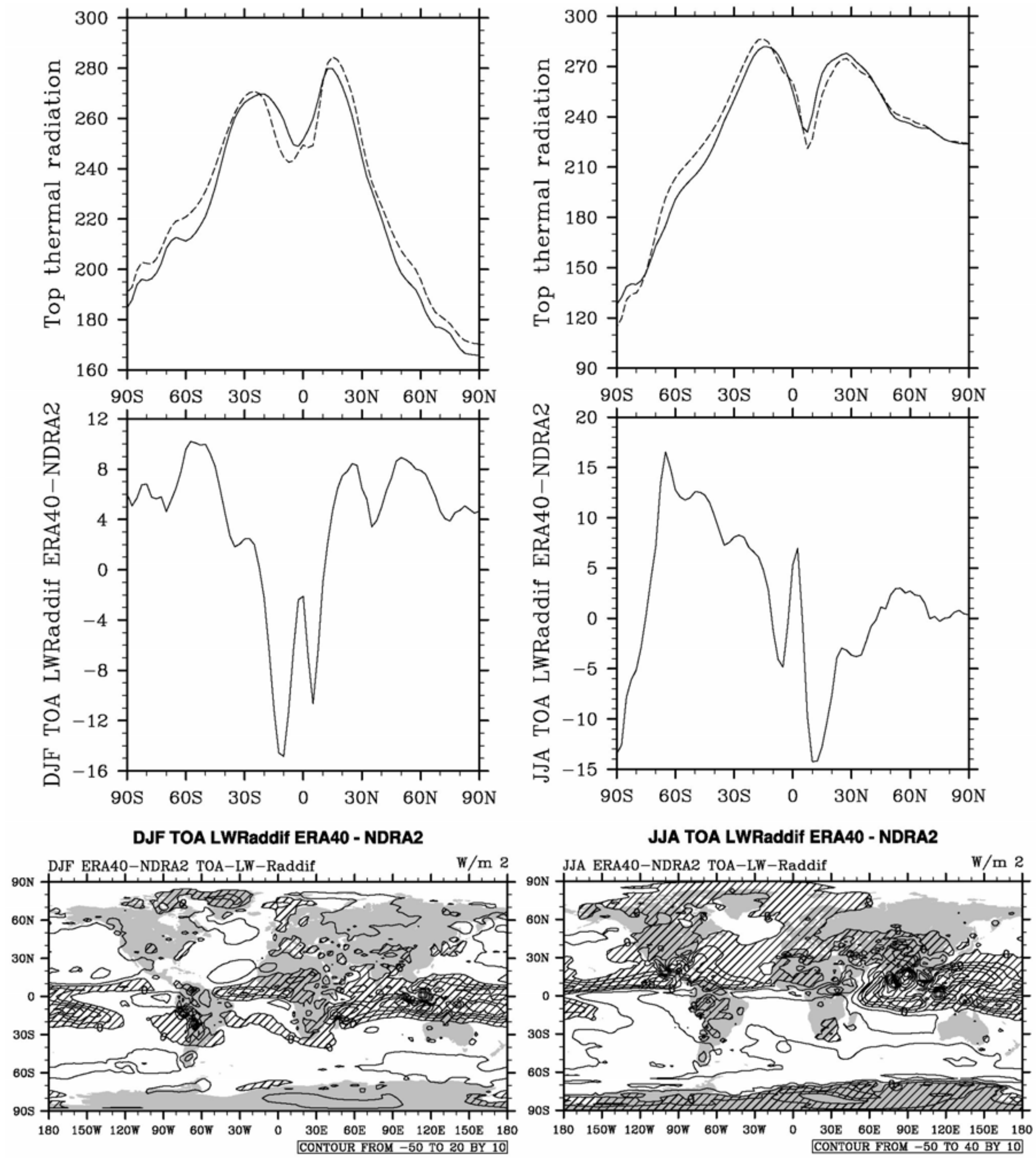

Fig. 2. Similar to fig. 1, except showing longwave upward radiative flux at the top of the atmosphere. Units are W m^{-2} and contour interval is 10 W m^{-2}. Large differences (up to 25%) occur near much of the ICZ and SPCZ.

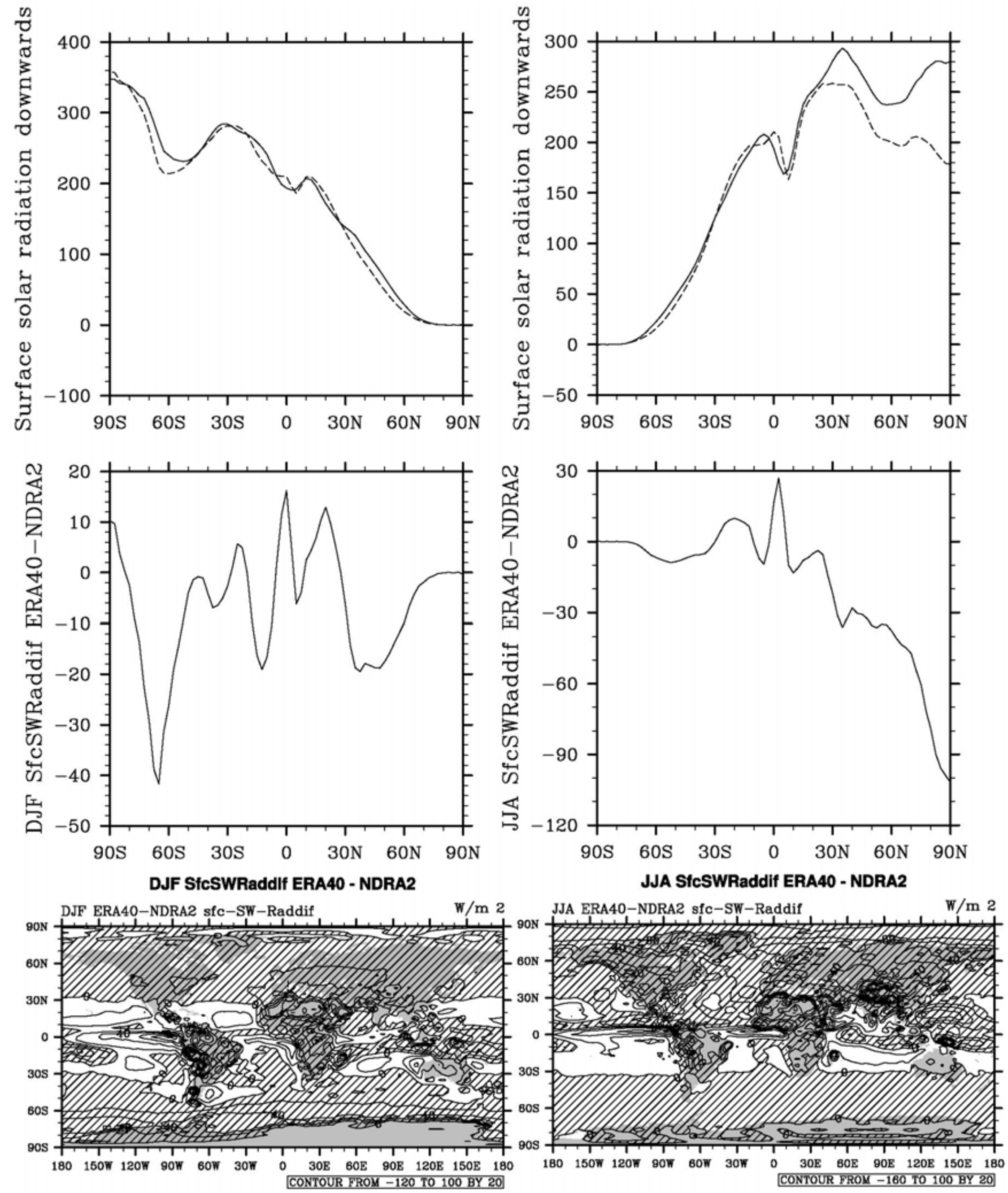

Fig. 3. Similar to fig. 1, except showing short wave radiative flux reaching the surface. Units are W m^{-2} and contour interval is 20 W m^{-2}. Notable differences occur near the ICZ and SPCZ and high latitudes of the summer hemisphere.

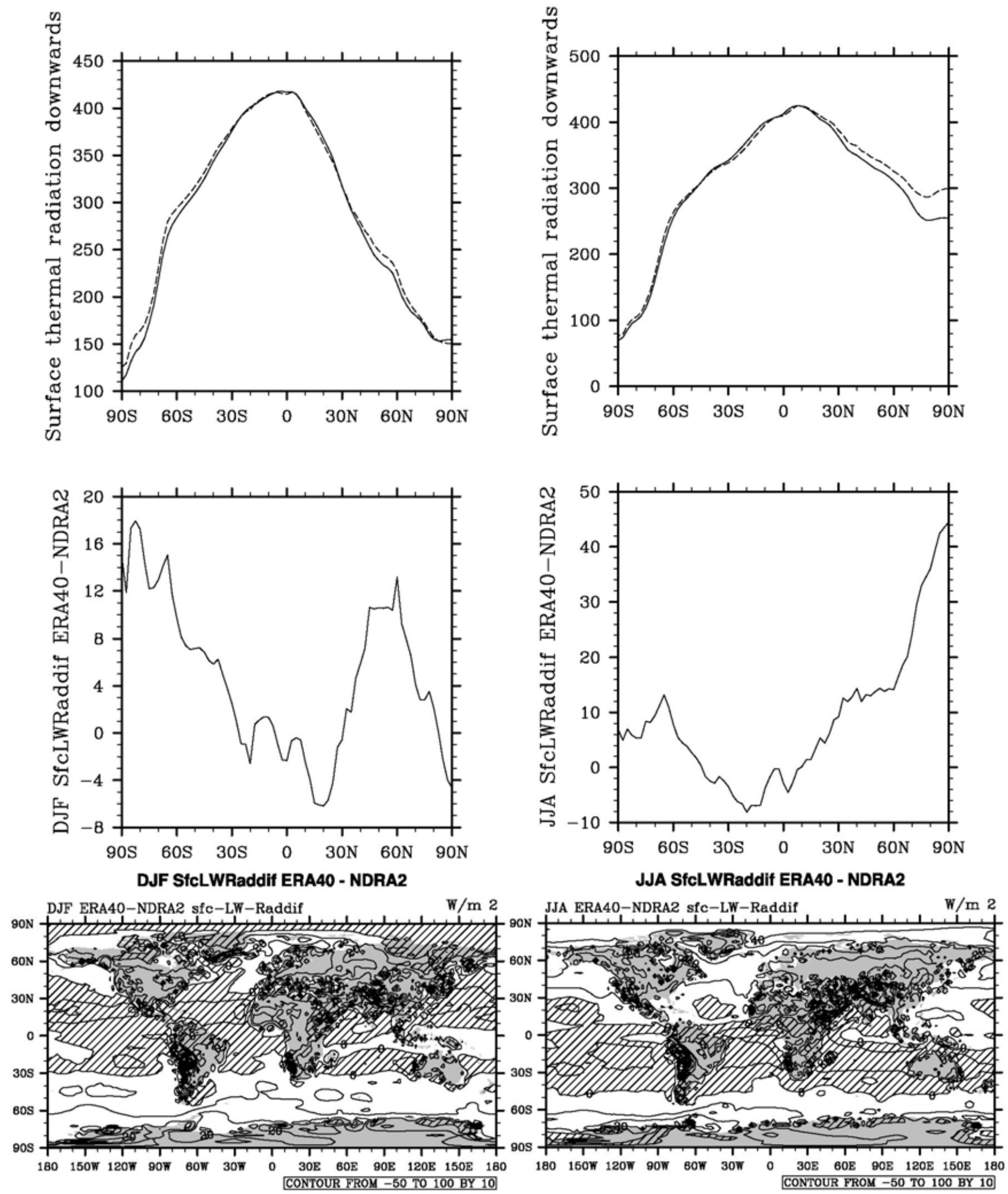

Fig. 4. Similar to fig. 1, except showing surface longwave radiative flux. Units are W m^{-2} and contour interval is 10 W m^{-2}. Notable differences occur near higher topography and polar land areas. Winter subtropical oceans have uniformly larger slwrf in NDRa2 data.

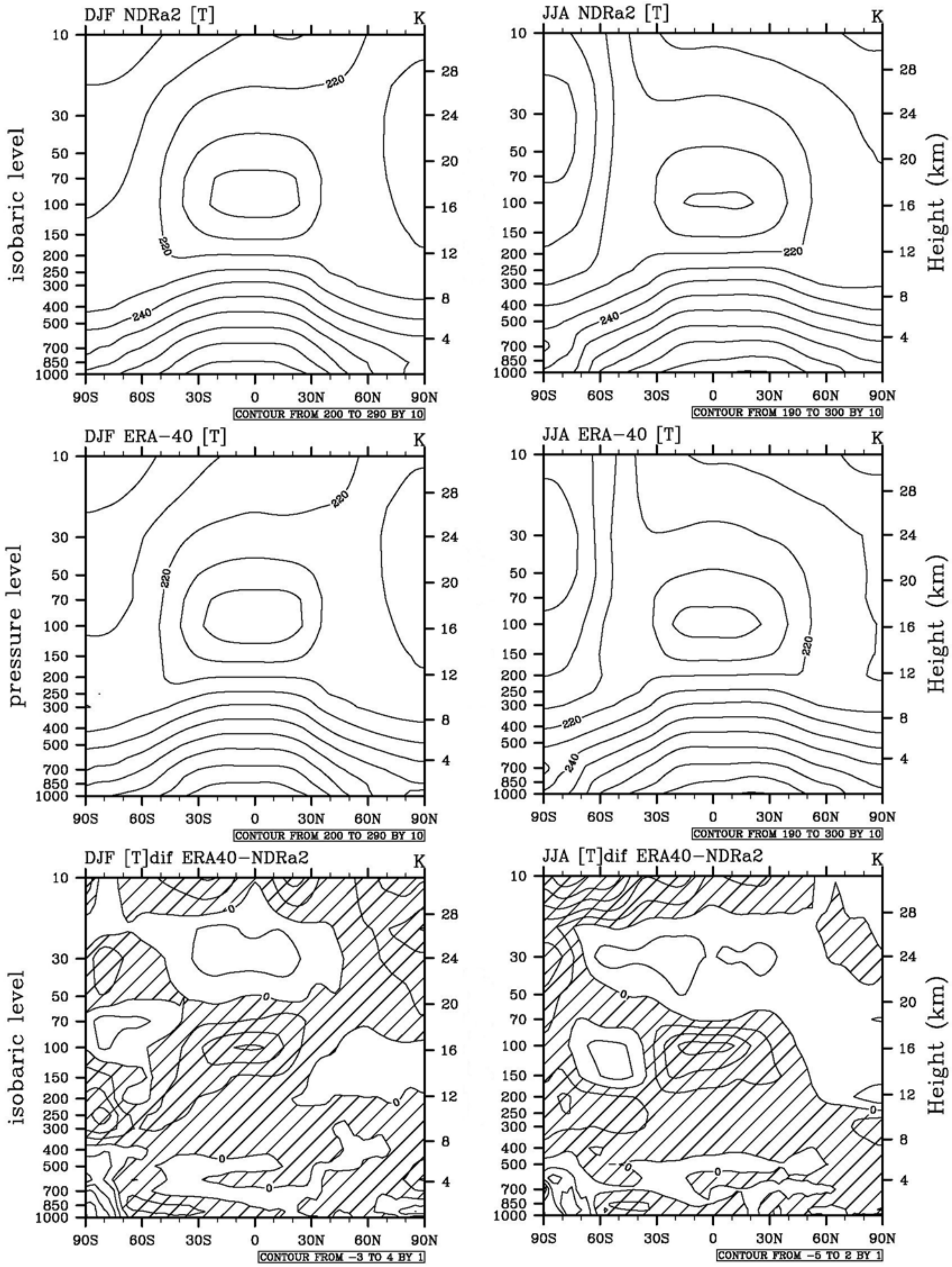

Fig. 5. Zonal mean temperature, [T]. NDRa2 data top row, ERA40 data middle row, difference: ERA40 minus NDRa2 bottom row. Left column DJF, right column JJA. Contour interval is 10 K for top and middle row, 1 K for bottom row. Negative values (ERA40 cooler) are shaded. Tropical tropopause and lower level Southern Hemisphere midlatitudes are colder in ERA40 data.

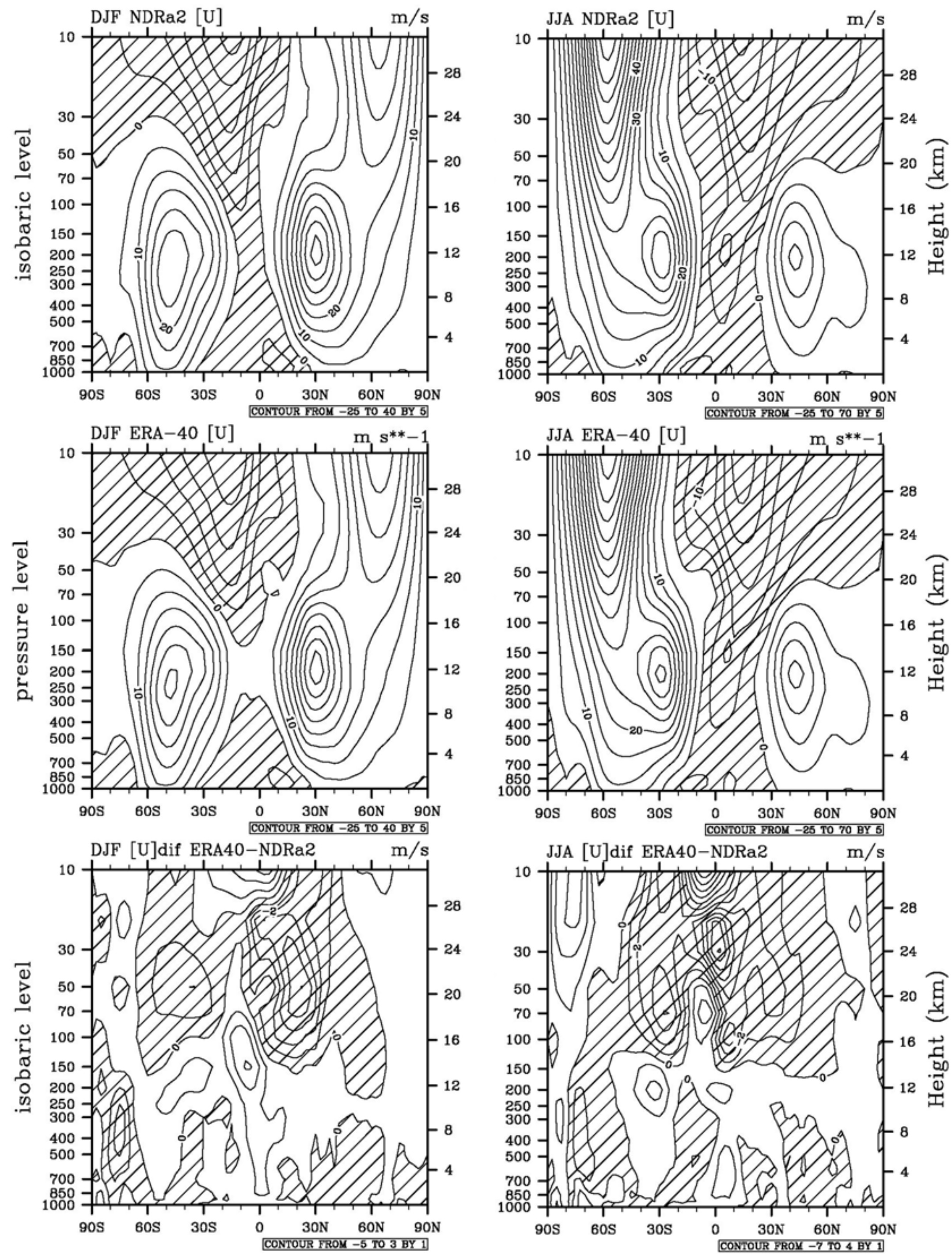

Fig. 6. Similar to fig. 5 except showing zonal mean zonal wind, [U]. ERA40 has equatorial, upper tropospheric westerlies not seen in other datasets during DJF. Larger differences occur in the stratosphere, where ERA40 data often have stronger easterlies in middle stratosphere, weaker near equatorial tropopause. Stratospheric winter polar night jet is stronger in ERA40 data. Contour interval is 5 m/s for top and middle row, 1 m/s for bottom row. Shaded areas indicate negative values (easterlies).

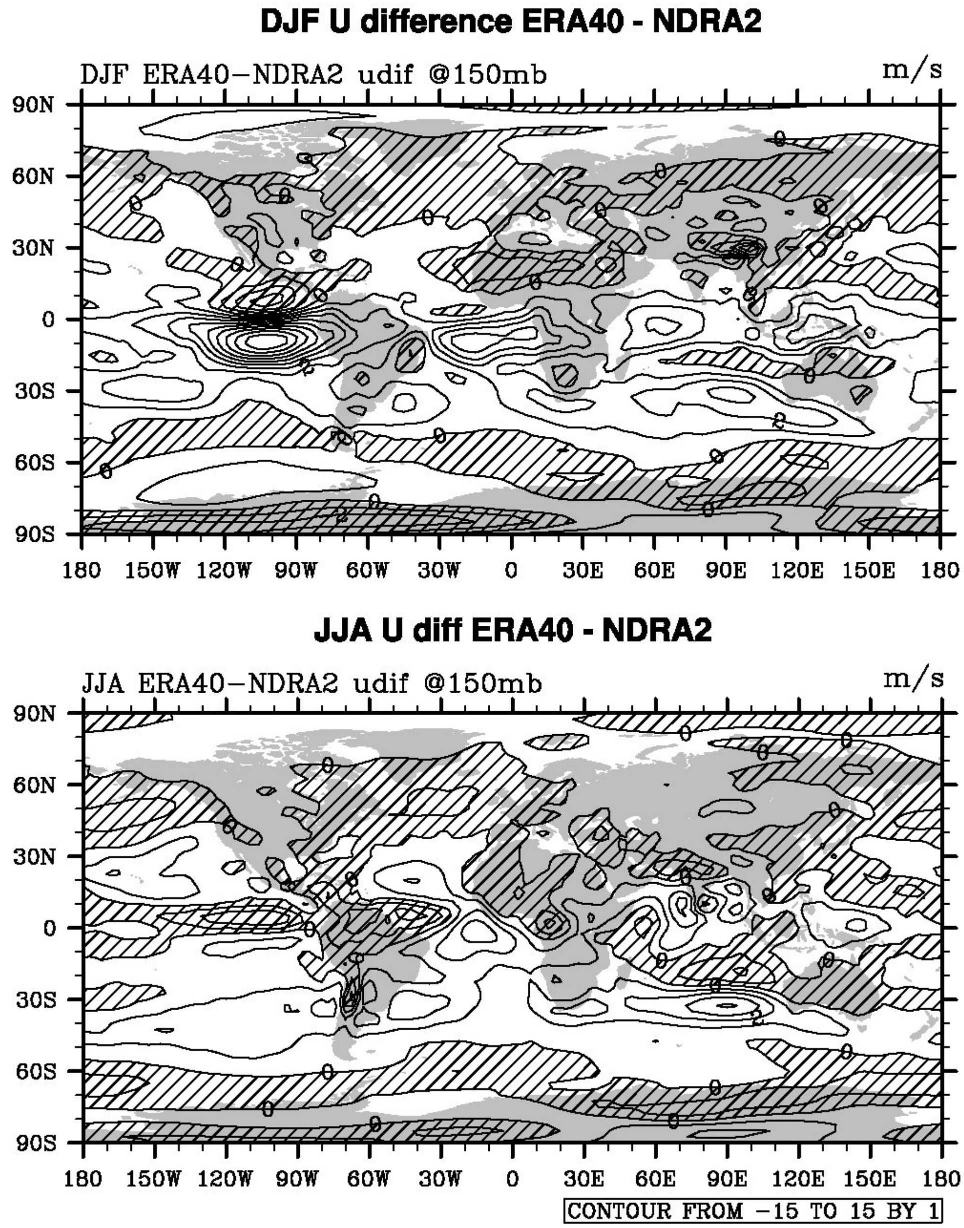

Fig. 7. Geographic distribution of zonal wind difference, ERA40 minus NDRa2 at 150 hPa for DJF (top) and JJA (bottom). Contour interval is 1 m/s. Shaded areas are where the difference is negative. Larger differences occur over the tropical Atlantic and eastern tropical Pacific. In DJF, NDRa2 data have stronger easterlies over Atlantic and across Indian oceans; in ERA40, region of westerlies is wider longitudinally in tropical Atlantic.

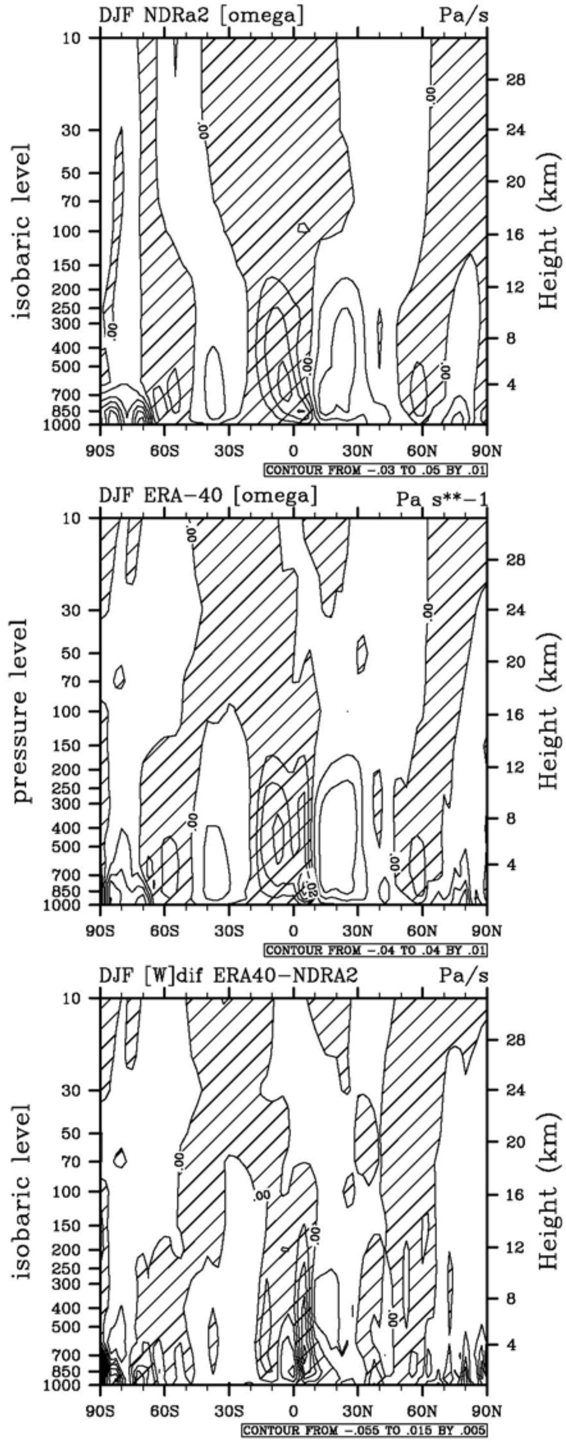

Fig. 8. Similar to the left column of fig. 5, except for zonal mean cross sections of pressure velocity (ω = dP/dt). Contour interval is 0.01 Pa/s for top and middle plot, 0.005 for the difference field (bottom plot); shaded areas indicate negative values (upward motion). ERA40 has a "second" peak rising zone near 5 N in [ω] that is not apparent in NDRa2 data.

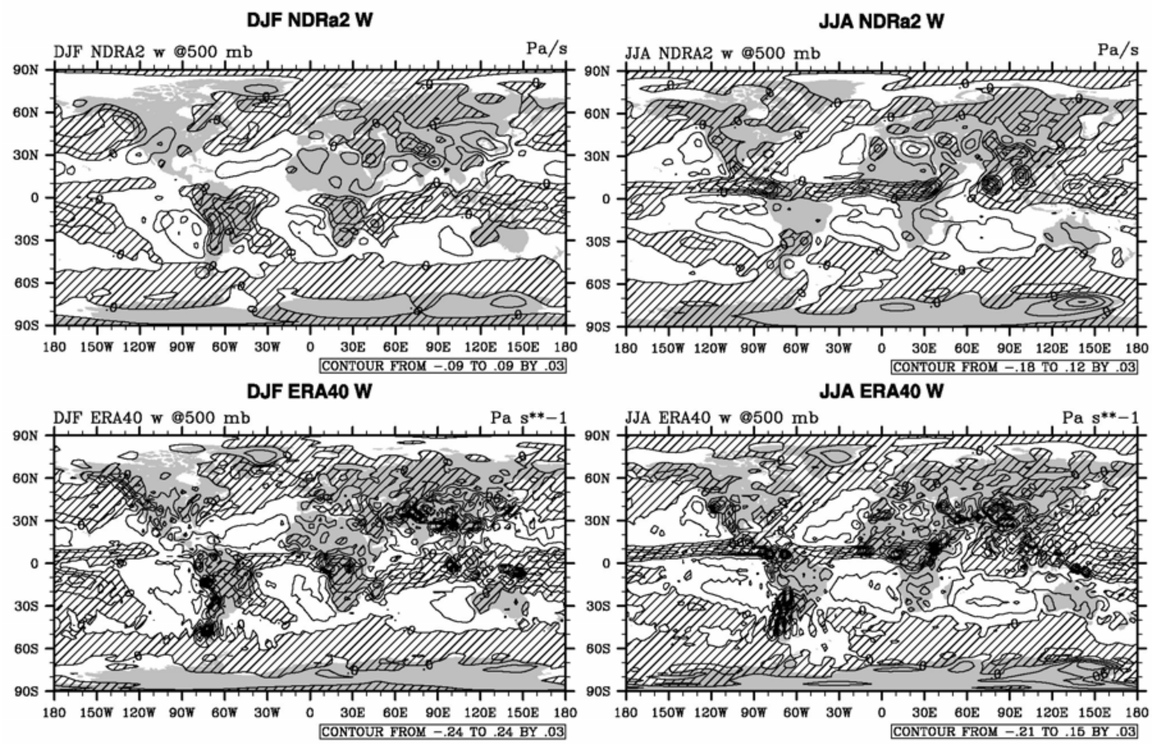

Fig. 9. Comparison plots of time mean pressure velocity (ω = dP/dt) for NDRa2 data (top row) and ERA40 data (bottom row) during DJF (left column) and JJA (right column). Despite using the same grid, the NDRa2 data tend to have broader features such as parts of the ICZ. NDRa2 data have very weak ICZ in the central Atlantic and weaker ICZ in the east Pacific than ERA40 during DJF. The Atlantic and east Pacific ICZ is at a higher latitude than many other regions, consequently, ERA40 data have the 'second' peak rising zone mentioned in previous figure. Near steep-sloped topographic features, such as the Himalayas and the Andes ω has more waviness in ERA40 data. Contour interval is 0.03 Pa/s; shaded areas indicate negative values (upward motion).

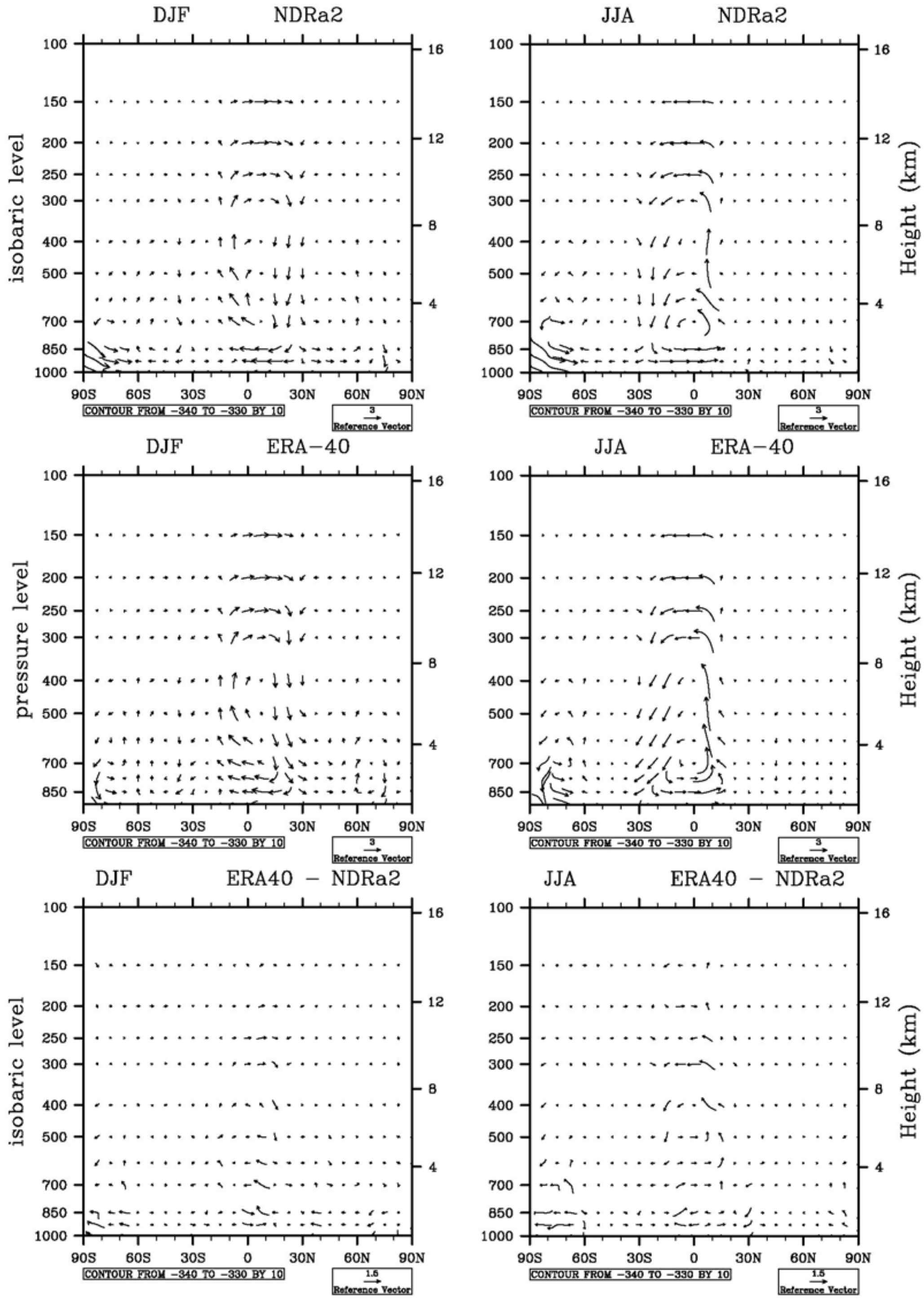

Fig. 10. Similar to fig. 5 except using vectors to show the zonal mean circulation in the meridional and vertical plane.

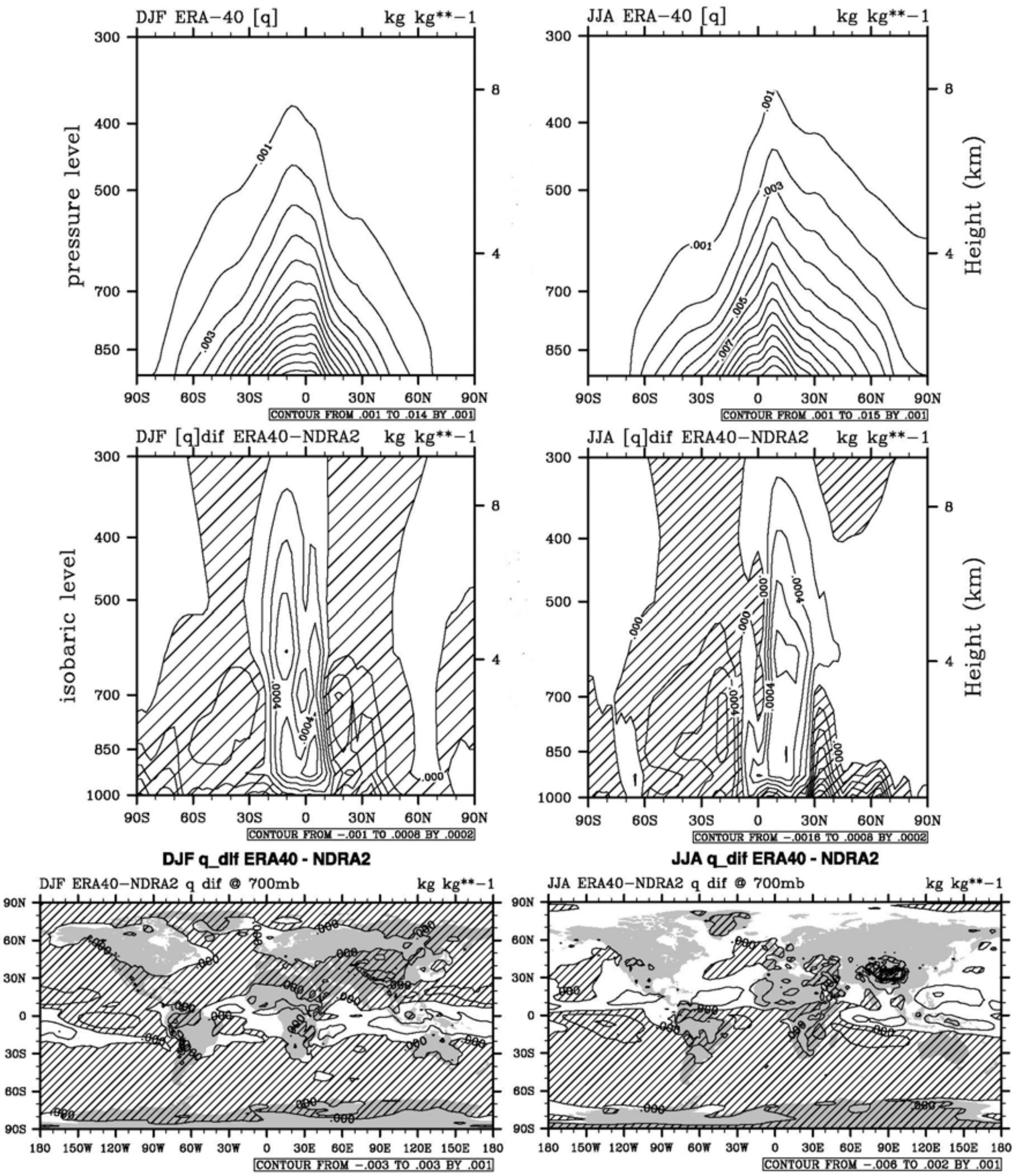

Fig. 11. Zonal mean specific humidity [q] ERA40 data top row, [q] difference: ERA40 minus NDRa2 middle row, bottom row is difference in q, ERA40 minus NDRa2 at 700 hPa level. Left column DJF, right column JJA. Contour interval is 1 gm/kg for top and bottom rows, 0.2 gm/kg middle row. Negative values are shaded. Distribution of [q] for NDRa2 very similar in appearance to top row. ERA40 has higher q than NDRa2 along most of the ICZ, lower in much of the winter hemisphere subtropics.

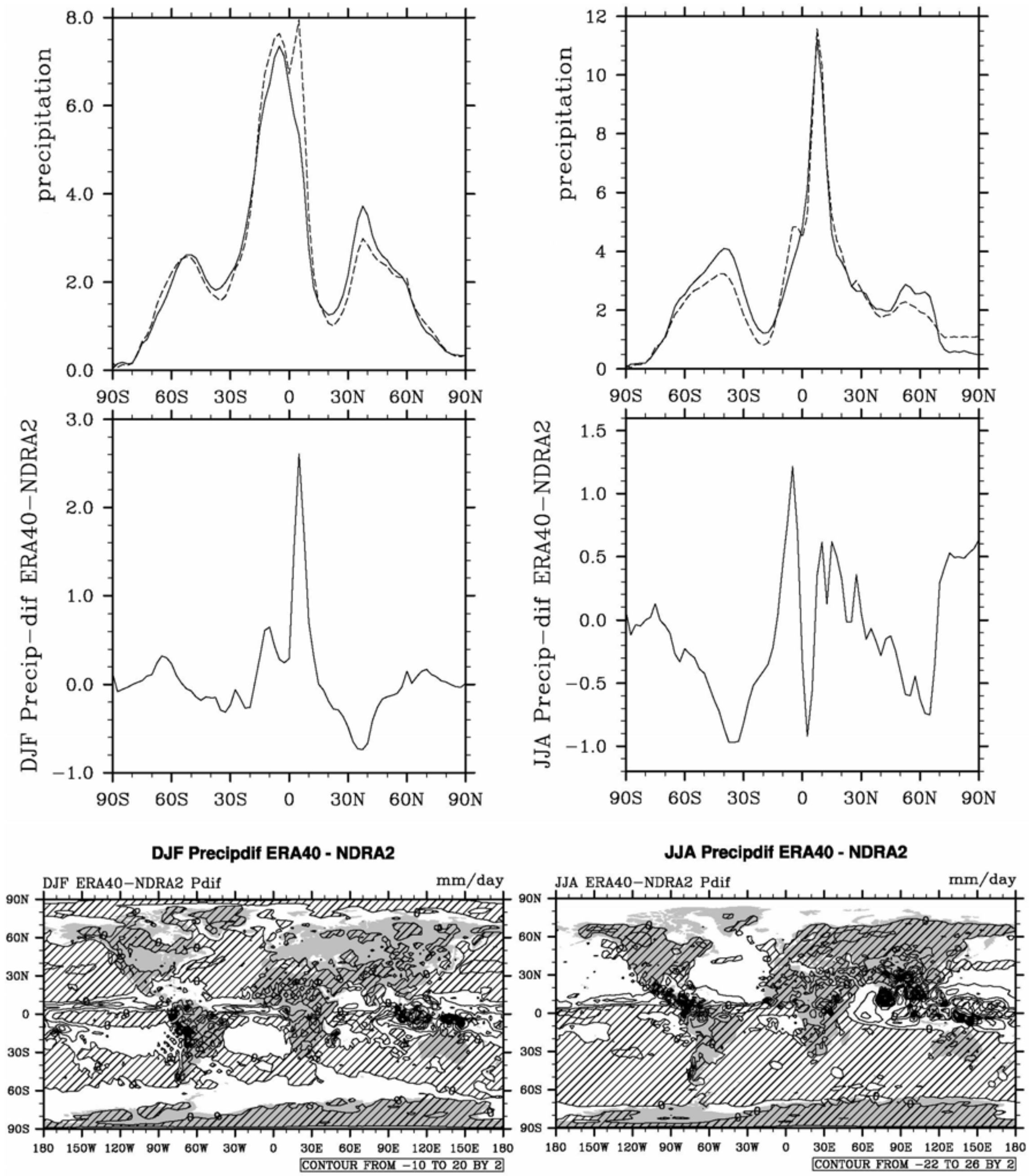

Fig. 12. Similar to fig. 1 except showing precipitation rate, P. Units are mm/day and the contour interval is 2 mm/day. ICZ in Atlantic and eastern Pacific has greater P in ERA40. In contrast, NDRa2 data has larger ICZ-associated P in Indian and west Pacific oceans. During winter, P in midlatitude storm tracks is generally less in ERA40. During JJA, less P in ERA40 over northern continents.

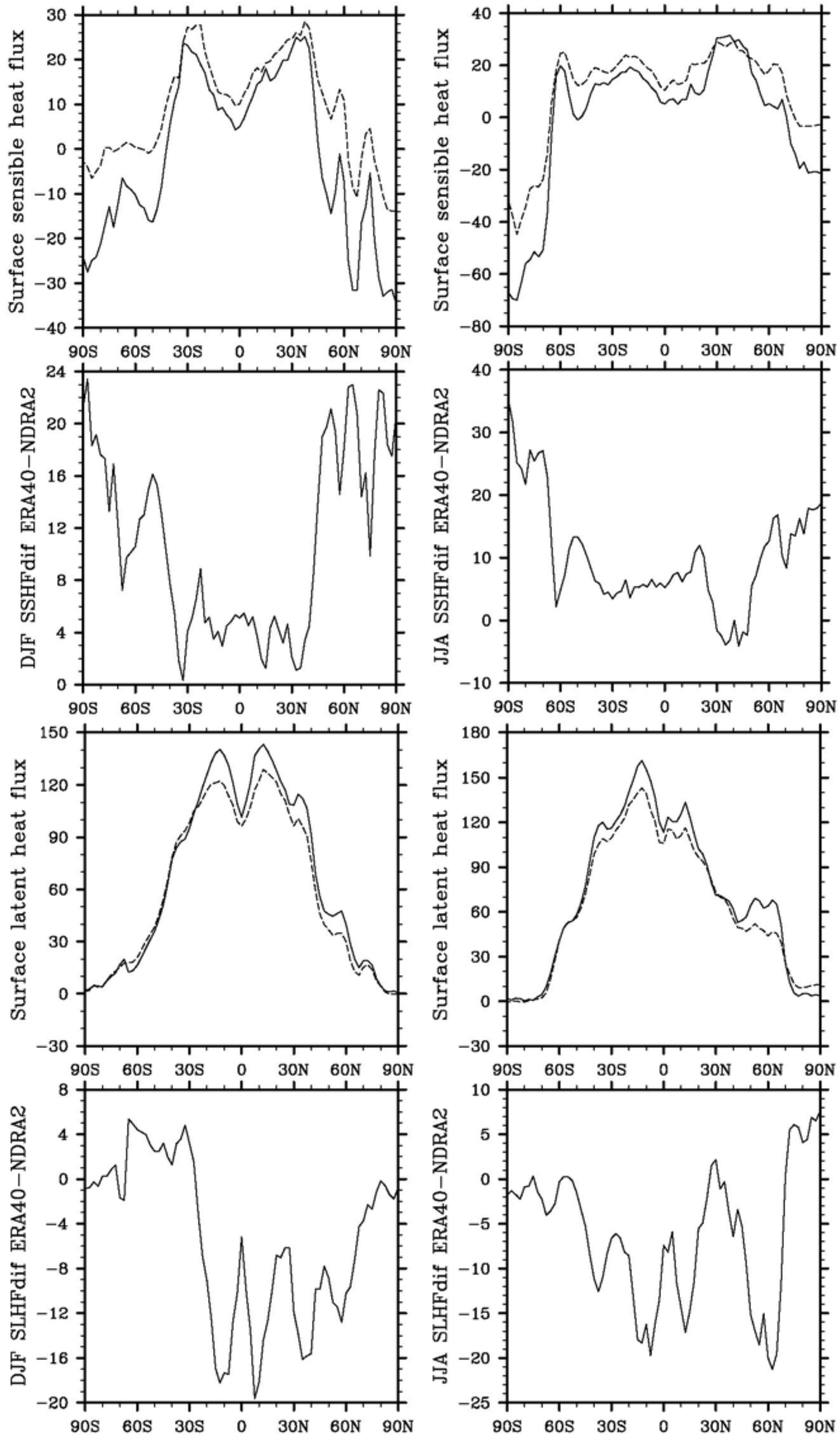

Fig. 13. Zonal mean surface sensible heat flux, [SHF] and ERA40 minus NDRa2 difference (top and second row, respectively). Zonal mean surface latent heat flux, [LHF] and ERA40 minus NDRa2 difference (third and bottom row, respectively). In top and third rows: solid line is NDRa2; dashed line is ERA40. Units are W m^{-2}.

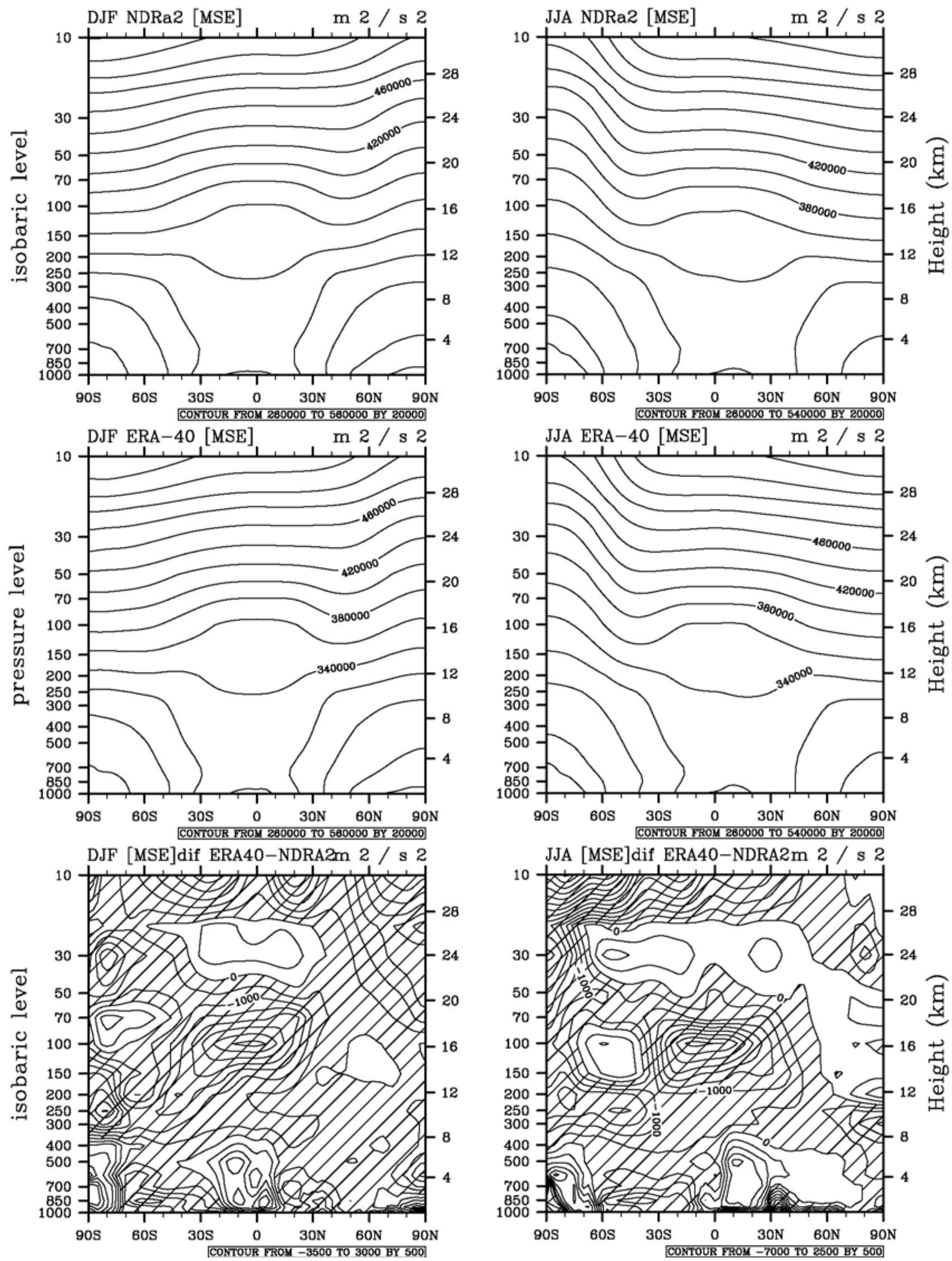

Fig. 13. Similar to fig. 5 except for zonal mean moist static energy, [MSE]. Contour interval is 20 000 $m^2 s^{-2}$ except for bottom row which uses interval 500 $m^2 s^{-2}$. Low level tropical differences reflect greater moisture present in ERA40 data; tropical tropopause and southern hemisphere low level midlatitudes regions differences reflect cooler ERA40 temperatures there.

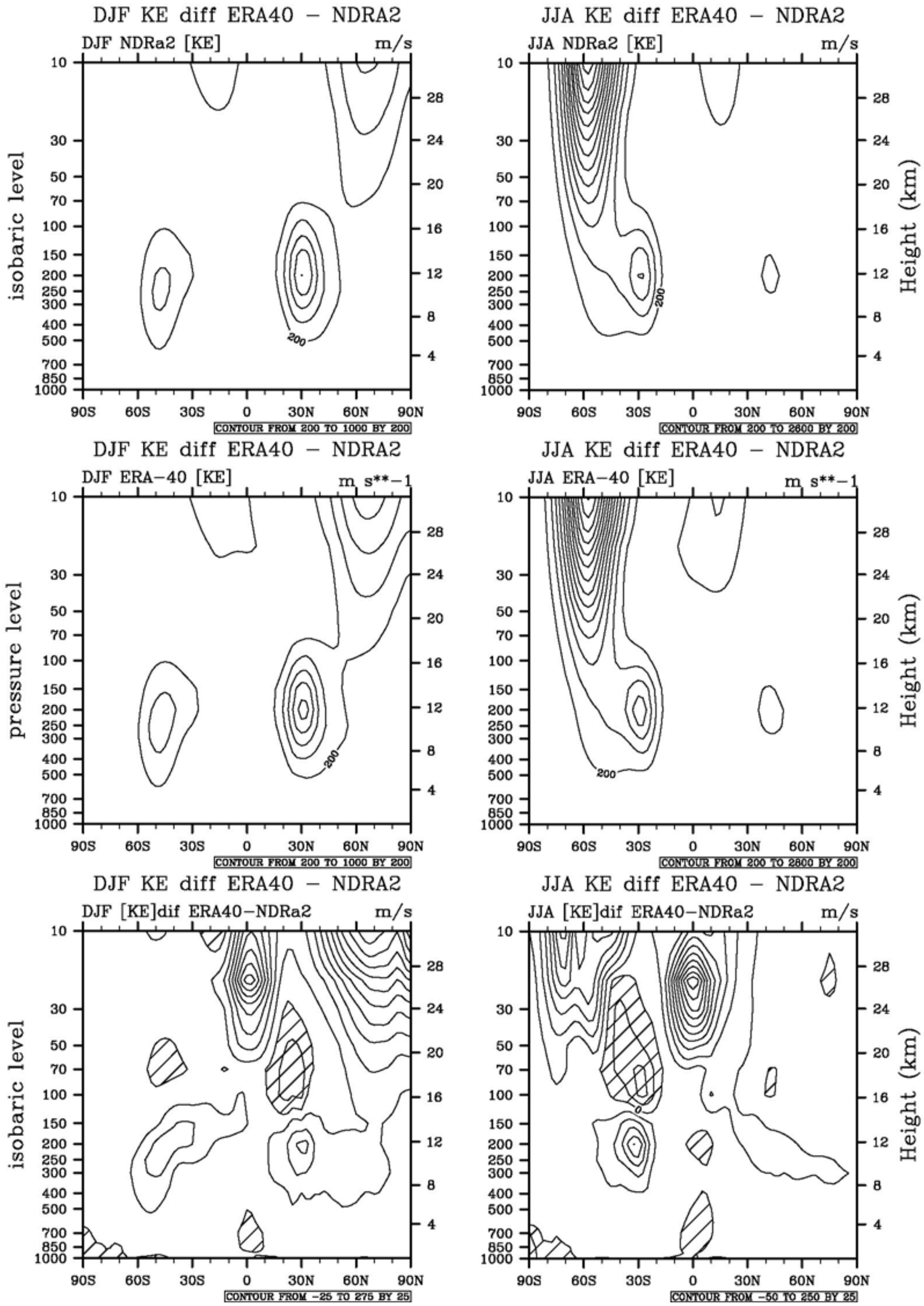

Fig. 14. Similar to fig. 5 except for zonal mean kinetic energy, [KE]. Contour interval is 200 $m^2 s^{-2}$ except for bottom row which uses interval 25 $m^2 s^{-2}$. ERA40 data generally have more [KE] especially in winter stratosphere, winter subtropical jet, and tropical stratosphere.